DISSERTATION

Molecular Mechanisms of Nephroprotection of SGLT2 Inhibitor

Molekulare Mechanismen der Nephroprotektion von SGLT2 Hemmern

zur Erlangung des akademischen Grades
Doctor medicinae (Dr. med.)

vorgelegt der Medizinischen Fakultät
Charité – Universitätsmedizin Berlin

von

Xin Chen

Erstbetreuung: Prof. Dr. med. Stanislao Morgera

Datum der Promotion: 20.06.2025

Table of contents

List of tables

List of figures

List of abbreviations

Abbreviations	
CKD	Chronic kidney disease
SGLT2	Sodium-glucose cotransporter 2
5/6 Nx	Five-sixths nephrectomy
TGF	Tubuloglomerular feedback
GBM	Glomerular basement membrane
mTORC1	Rapamycin complex 1
AMPK	5' AMP-activated protein kinase
NLRP3	Inflammasome
IL	Interleukin
TNF-α	Tumour necrosis factor-α
FGF-2	Fibroblast growth factor 2
TGF-β	Transforming growth factor beta
T2DM	Type 2 diabetes mellitus
eGFR	Estimated glomerular filtration rate
qRT-PCR	Quantitative real-time polymerase chain reaction
Uni-Nx	Uni-nephrectomy of the right kidney
Sham	Sham operation
PBO	Placebo
TELM	Telmisartan
EMPA	Empagliflozin
MC	Metabolic cages
OP1	Operation 1
OP2	Operation 2

BP	Blood pressure
ACR	Urinary albumin-to-creatinine ratio
Ccr	Creatinine clearance
PAS	Periodic acid–schiff staining
PASM	Periodic schiff-methenamine staining
Masson	Masson’s trichrome staining
DAPI	4',6-Diamidino-2-phenylindole
RFU	Relative fluorescence units
mRNA	Messenger RNA
DEGs	Differentially expressed genes
C1QA	Complement Component 1, Q Subcomponent, A Chain
C1QC	Complement Component 1, Q Subcomponent, C Chain
FMOD	Fibromodulin
REN	Renin
FMO2	Flavin Containing Dimethylaniline Monoxygenase 2
RPL36	Ribosomal Protein L36
ANOVA	One-way analysis of variance
ATP	Adenosine triphosphate
RAAS	Renin-angiotensin-aldosterone system
C1Q	Complement Component 1, Q Subcomponent
DAMPs	Damage-associated molecular patterns
C3a	Complement Component 3a
C5a	Complement Component 5a
C5b	Complement Component 5b
PDGF	Platelet-derived growth factor

EndMT	Endothelial-to-mesenchymal
PMT	Pericyte-to-myofibroblast
GFR	Glomerular filtration rate

Abstract

Abstract (English)

Introduction: It is now widely accepted that the nephroprotective effects of sodium-glucose cotransporter 2 (SGLT2) inhibitors are attributed to their glucose-lowering effect. Some recent studies suggest that SGLT2 inhibitors have potential nephroprotective effects beyond glucose-lowering; however, these mechanisms are unclear.

Methods: Male Wistar rats with 5/6 nephrectomy (5/6Nx) were used to investigate the effect of empagliflozin in non-diabetic chronic kidney disease (CKD) rats. Five groups were established: Sham + placebo, 5/6Nx + placebo; 5/6Nx + telmisartan (5 mg/kg/day), 5/6Nx + empagliflozin (3 mg/kg/day); 5/6Nx + empagliflozin (15 mg/kg/day). Medication or a placebo was administered daily via oral gavage for 95 days. RNA sequencing and quantitative real-time polymerase chain reaction (qRT-PCR) were used to investigate the underlying mechanism.

Results: 5/6Nx caused a significant increase in serum creatinine and urinary albumin excretion rate (ACR), along with severe glomerulosclerosis and renal interstitial fibrosis in rats. Empagliflozin demonstrated a dose-dependent positive effect on ACR and creatinine clearance (Ccr) change from baseline. Both high and low doses of empagliflozin improved renal histological injury indicators, such as renal interstitial fibrosis, perivascular fibrosis, and glomerulosclerosis. The substantial reduction in 5/6Nx-induced urinary adenosine excretion rate, a surrogate parameter of the tubuloglomerular feedback mechanism (TGF), was improved only in the high-dose empagliflozin treatment group ($p<0.05$), suggesting that empagliflozin dose-dependently corrects the 5/6Nx-induced impaired TGF. Furthermore, the final urinary adenosine excretion was positively related to final Ccr and negatively related to renal interstitial fibrosis. However, according to immunofluorescence analysis, empagliflozin did not affect CD8+ T cells, CD4+ T cells, or CD68+ cells (macrophages). Importantly, RNA sequencing and qRT-PCR revalidation indicated that 5/6Nx resulted in upregulation of complement component 1Q subcomponent A chain (*C1QA*) as well as complement component 1Q subcomponent C chain (*C1QC*) gene expression, which was attenuated by empagliflozin treatment.

Conclusion: Empagliflozin improves renal function and mitigates renal fibrosis in non-diabetic CKD through dose-dependent activation of TGF and suppression of complement system activation.

Zusammenfassung (Deutsch)

Einleitung: Es ist inzwischen allgemein anerkannt, dass die nephroprotektive Wirkung von Natrium-Glukose-Cotransporter 2 (SGLT2) Inhibitoren auf seine glukosesenkende Wirkung zurückzuführen ist. Einige neuere Studien deuten darauf hin, dass SGLT2-Inhibitoren potenziell nephroprotektive Wirkungen haben, die über die Glukosesenkung hinausgehen; diese Mechanismen sind jedoch noch nicht klar.

Methoden: Männliche Wistar-Ratten mit 5/6-Nephrektomie (5/6Nx) wurden verwendet, um die Wirkung von Empagliflozin bei nicht-diabetischen Ratten mit chronischer Nierenerkrankung (CKD) zu untersuchen. Es wurden fünf Gruppen gebildet: Scheinbehandlung + Placebo, 5/6Nx + Placebo; 5/6Nx + Telmisartan (5 mg/kg/Tag), 5/6Nx + Empagliflozin (3 mg/kg/Tag); 5/6Nx + Empagliflozin (15 mg/kg/Tag). Das Medikament oder Placebo wurde täglich über eine orale Schlundsonde über 95 Tage verabreicht. RNA-Sequenzierung und quantitative Echtzeit-Polymerase-Kettenreaktion (qRT-PCR) wurden eingesetzt, um die potenziell zugrunde liegenden Mechanismen zu untersuchen.

Ergebnisse: 5/6Nx verursachte bei Ratten einen signifikanten Anstieg des Serumkreatinins und der Albuminausscheidungsrate im Urin (Albumin Creatinine Ratio, ACR) sowie eine schwere Glomerulosklerose und interstitielle Nierenfibrose. Empagliflozin zeigte eine dosisabhängige positive Wirkung auf die ACR und die Veränderung der Kreatinin-Clearance (Ccr) gegenüber dem Ausgangswert. Beide Dosierungen von Empagliflozin verbesserten die Parameter der histologischen Nierenschädigung, sowie die interstitielle Nierenfibrose, die perivaskuläre Fibrose und die Glomerulosklerose. Die erhebliche Verringerung der 5/6Nx-induzierten Adenosinausscheidungsrate im Urin, ein Surrogatparameter des tubuloglomerulären Rückkopplungsmechanismus (TGF), wurde nur in der hochdosierten Empagliflozin-Behandlungsgruppe verbessert ($p<0{,}05$), was darauf hindeutet, dass Empagliflozin dosisabhängig die 5/6Nx-induzierte TGF Beeinträchtigung korrigiert. Außerdem korrelierte die endgültige Adenosinausscheidung im Urin positiv mit der endgültigen Ccr und negativ mit der interstitiellen Nierenfibrose. Eine ebenfalls stattgehabte Immunfluoreszenzanalyse ergab das Empagliflozin keine Auswirkungen auf CD8+ T-Zellen, CD4+ T-Zellen und CD68+ Zellen (Makrophagen), hatte. Eine RNA-Sequenzierung mit anschließender qRT-PCR-Revalidierung ergab, dass 5/6Nx zu einer Hochregulierung der Genexpression der Komplementkomponente 1Q Subkomponente

A-Kette (*C1QA*) sowie der Komplementkomponente 1Q Subkomponente C-Kette (*C1QC*) führte, die durch die Empagliflozin-Behandlung abgeschwächt wurde.

Schlussfolgerung: Empagliflozin verbessert die Nierenfunktion und mildert die Nierenfibrose bei nichtdiabetischer CKD durch dosisabhängige Aktivierung von TGF und Abschwächung der Aktivierung des Komplementsystems.

1. Introduction

1.1 The pathophysiology of chronic kidney disease

Chronic kidney disease (CKD) is caused by irreversible changes in the kidney's function and structure over months or years due to pathogenic factors, including exogenous toxins, primary kidney disease, and chronic diseases such as diabetes(1). Despite the diverse etiology of CKD, they all culminate in progressive glomerulosclerosis, tubular atrophy, and interstitial fibrosis(1). Tubuloglomerular feedback (TGF) and inflammation play a vital role in these pathological processes.

1.2 Impaired TGF promotes renal fibrosis in CKD

TGF is an essential mechanism in renal physiology for maintaining individual intra-glomerular pressure and filtration rate. The mechanism of TGF is that macula densa located in the thick ascending branch of the loop of Henle senses changes in urinary sodium concentration and activate adenosine-mediated signaling feedback to adjust the vascular tone of the glomerular afferent arterioles(2). Impaired TGF leads to increased intra-glomerular pressure as well as tubular overload. In CKD, endogenous or exogenous pathogenic factors lead to focal glomerular loss and its corresponding TGF inactivation, resulting in increased filtration pressure and abnormal TGF response in the residual renal units(3). Prolonged elevated intraglomerular pressure and hyperfiltration induce renal inflammation and fibrosis, which are important factors in chronic progressive renal unit loss. The mechanical stress induced by intracapillary hypertension causes the glomerular basement membrane (GBM) to expand and forces adaptive hypertrophy or even shedding of the podocytes covering the GBM surface, which exacerbates glomerular hyperfiltration and promotes capillary adhesion to the Bowman's capsule(4). Tubular pressure overload from glomerular hyperfiltration can lead to tubular dilatation and hypertrophy of the tubular epithelium. More seriously, the overload of solutes activates various reabsorption transporters in the tubule and affects intracellular signalling. One example is increased amino acid reabsorption, and consequently activation of the mammalian target of rapamycin complex 1 (mTORC1) pathway, which induces renal hypertrophy(5). The overabundance of glucose as a solute causes the upregulation of glucose transporters which in turn inhibits the 5' AMP-activated protein kinase (AMPK) signalling pathway(6). The altered signalling and, consequently elevated oxygen consumption caused by tubular reabsorption overload drives tubulointerstitial inflammation, hypoxia, and fibrosis(6). In summary, reducing intra-glomerular pressure and hyperfiltration in the residual renal unit by modulating TGF is likely to retard the progression of CKD.

1.3 Inflammation and fibrosis in CKD

The key factors contributing to CKD injury and repair are immune cells, inflammatory cytokines, and the complement system. After kidney injury, the release of various cellular components from damaged or necrotic cells and the accumulation of large amounts of toxins activate various cells expressing Toll-like receptors, such as renal tissue-resident cells (renal tubular epithelial cells, endothelial cells, fibroblasts) or recruited immune cells (monocytes, macrophages, lymphocytes), thereby promoting complement system activation, inflammasome (NLRP3) formation and secretion of pro-inflammatory factors such as interleukin-1α (IL-1α), interleukin-1β (IL-1β) and interleukin-6 (IL-6)(7, 8). This inflammation induced after kidney injury is a protective response that aims to eliminate the factors of injury and establish tissue repair, but the persistent inflammation recruits and activates myofibroblasts, leading to glomerular and interstitial fibrosis. Macrophages, which differentiate into pro- and anti-inflammatory cell subtypes, play an important role in this process. Monocytes recruited to the site of injury differentiate into different subtypes of macrophages, mainly pro-inflammatory M1 macrophages and anti-inflammatory M2 macrophages, in response to stimulation by different cytokines. M1 macrophages produce a variety of pro-inflammatory molecules such as IL-6 and tumor necrosis factor-α (TNF-α) to maintain and expand renal inflammation, while M2 macrophages produce anti-inflammatory cytokines and promote renal tubular regeneration and repair(9). However, activated M2 macrophages also release transforming growth factor beta (TGF-β), which induce proliferation and conversion of fibroblast-type cells to myofibroblasts, thereby promoting renal fibrosis(9). In addition to macrophages, many cells are recruited to the impaired glomeruli and tubular mesenchyme. The recruited CD4+ T cells release interleukin-17 to induce the expression of cytokines and chemokines in proximal tubular epithelial cells. It has been proposed that administering depleted CD4 antibodies prevents renal fibrosis while transferring CD4+ T cells into lymphocyte-deficient mice restores renal fibrosis(10). Cytotoxic T cells (CD8+ T cells) are involved in renal fibrosis by secreting interferon-γ. One study revealed that CD8+ T cells and interferon-γ reduced the CD4+ T cell-induced transformation of monocytes to fibroblasts(11).

1.4 Effects of Sodium-glucose cotransporter 2 inhibitors on kidney

Sodium-glucose cotransporter 2 (SGLT2) is mainly located in the initial segment of the proximal renal tubule and reabsorbs more than 90% of the sodium and glucose in the tubule(12), therefore blocking SGLT2-mediated sodium/glucose reabsorption at the renal tubule using SGLT2 inhibitors is effective in reducing blood glucose. Recently, SGLT2 inhibitors, such as empagliflozin, canagliflozin, dapagliflozin, and ertugliflozin, have been approved for the purpose of treating type 2 diabetes mellitus (T2DM). Interestingly, subsequent controlled clinical trials to test the safety of SGLT2 inhibitors have revealed that SGLT2 inhibitors are not only effective in reducing blood glucose levels but also in improving cardiac and renal function in patients. The EMPA-REG OUTCOME Clinical Trials(13) showed beneficial effects of empagliflozin beyond the necessary safety parameters, including reducing macroalbuminuria, inhibiting the rise in serum creatinine, and preventing a decrease in estimated glomerular filtration rate (eGFR). Initially, it was widely believed that the improvement in renal function in diabetic patients was due to the hypoglycaemic effect of SGLT2 inhibitors. However, EMPEROR-Reduced Clinical Trials(14) and EMPEROR-Preserved Clinical Trials(15) conducted in heart failure patients without diabetes showed that empagliflozin treatment improved non-diabetic patients' cardiac and renal function. Subsequently, large controlled clinical trials in CKD patients without type 2 diabetes showed renal benefit from dapagliflozin, such as the DAPA-CKD Clinical Trials(16) in 4304 CKD patients demonstrating that dapagliflozin (10 mg once daily) was effective in protecting renal function in patients with and without T2DM. In addition, the EMPA-KIDNEY study in 6609 CKD patients suggested that empagliflozin treatment reduced the risk of renal deterioration(17). This evidence suggests that SGLT2 inhibitors may have reno-protective mechanisms beyond glycaemic control. In conjunction with our discussion of the significant pathobiological changes in CKD, SGLT2 inhibitors may have prevented renal deterioration by affecting the renal TGF or inflammatory response. Some animal experiments have provided evidence supporting this theoretical hypothesis(18), but studies show contradictory results (19). This may be due to the limitations of these studies, such as the use of diabetes models in many of them, the short duration of the interventions, and the fact that the use of a hypothesis-driven approach to assessing predefined pathways may overlook unknown mechanisms.

1.5 Investigating the effects of SGLT2 inhibitors on non-diabetic CKD rats

To clarify the nephroprotective effects of SGLT2 inhibitors and the mechanism, we established a non-diabetic CKD rat model using 5/6 nephrectomy to observe the impact of empagliflozin treatment for 95 days on renal function and morphology. Two doses of empagliflozin (3 mg/kg/d and 15 mg/kg/d) were set up to investigate the possible potential dose-dependence of SGLT2 inhibitors, and telmisartan was used as the gold standard for nephroprotection. To further explore the possible potential mechanism of SGLT2 inhibitors, RNA sequencing was used to search for SGLT2 inhibitors treatment-induced differentially expressed genes, which were subsequently validated by quantitative real-time polymerase chain reaction (qRT-PCR).

2. Methods

2.1 Experimental animals and protocol

Animal experiments were conducted with the consent of the Animal Care and Use Committee of Jinan University, Guangzhou, China (IACUC-20190830-02) and in accordance with the Guide for the Care and Use of Laboratory Animals published by the US National Institute of Health (NIH Publication No. 85-23, revised 1996).

7-week-old male Wistar rats were purchased from Vital River Laboratory Animal Technology Co., Ltd. Rats were housed at room temperature 22-25°C, humidity 55±5%, 12-h light/dark cycle and supplied with standard rat chow and water. After seven days of acclimatization, rats were randomly arranged into five groups: sham + placebo (10 animals); 5/6Nx + placebo (15 animals); 5/6Nx + telmisartan (5mg/kg/day, 15 animals); 5/6Nx + empagliflozin (3mg/kg/day, 15 animals); 5/6Nx + empagliflozin (15mg/kg/day, 15 animals). The random number method was used to group the animals as follows: Each animal was assigned a number from 1 to 70, and a random number generator was used to create a randomized sequence of these numbers. Animals corresponding to the first 10 numbers were assigned to the sham + placebo group, the next 15 to the following group, and so on until all animals were allocated to their respective groups. Five-sixths nephrectomy (5/6Nx) was performed under 2,2,2-tribromethanol (500mg/kg intraperitoneally) anaesthesia as follows: unilateral nephrectomy of the right kidney (Uni-Nx) at week 1, followed by amputation of both poles of the left kidney at week 3 (Figure 1), and all other operations except nephrectomy were conducted on rats in sham + placebo group. All rats received medication/placebo by gavage on day 1 immediately after surgery for 95 consecutive days until the end of the experiment (24h before euthanasia). Dose selection for telmisartan (20) and empagliflozin (21) was based on previous studies. Thereafter, the rats were weighed every 2 weeks and the medication dose was adjusted according to the latest body weight. Urine, blood, and blood pressure were collected at weeks 0 (Baseline), 7 (1 month after medication treatment) and 18 (the end), respectively (Figure 1). Blood pressure was measured by the tail-cuff technique (BP-2000 Blood Pressure Analysis System, model BP-2000-RP-4, Visitech Systems, U.S.A.). Urine collection was performed as follows: rats were individually placed in metabolic cages (MC) to collect 24-h urine and record 24-h urine volume. Baseline and week 7 blood samples were collected from the retro-orbital plexus under isoflurane (3%) chamber induced anaesthesia. The final blood sample (week 18) were collected from the abdominal aorta during the euthanasia process and placed in vacutainer (BD Vacutainer SST II Advance Serum Tube with Separating Gel and Clotting Activator). All blood samples were centrifuged at 3000 rpm for 10 min at 4°C and the supernatant was frozen at -80°C for further analysis. Urine was centrifuged at 12,000 rpm for 10 min at 4°C and the supernatant frozen at -80°C for further analysis. At week 18, rats were euthanized under 2,2,2-tribromethanol (500mg/kg intraperitoneally) anaesthesia, and blood and kidney samples were collected. After stripping the kidney envelope and weighing, the kidneys were cut in half longitudinally: 1/2 kidneys were fixed in 4% paraformaldehyde for further paraffin embedding; 1/2 kidneys were immersed in RNA Tissue Protection Reagent (No. 76106, Qiagen, Germany) and preserved at -80°C.

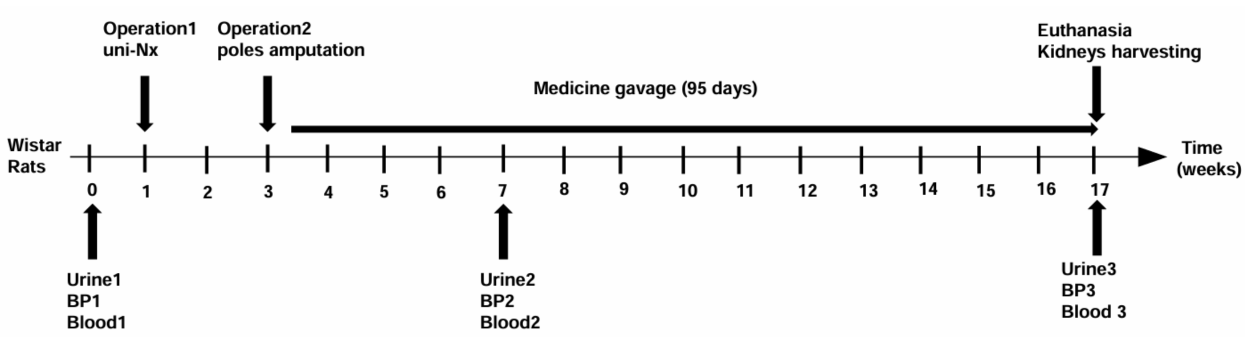

Figure 1: The time process of animal research. Uni-Nx: Unilateral nephrectomy of the right kidney; Poles amputation: Resection of both poles of left kidney; BP: Blood pressure; Blood 1 and Blood 2 were collected from retro-orbital venous plexus; Blood 3 was taken from the abdominal aorta. Citation: This figure has been modified from that in the paper - Chen, et al. 2023(22). The arrows for Urine3, BP3, Blood3, Euthanasia and Kidneys harvesting have been changed from 18 to 17 weeks.

2.2 Serum and urine analysis

Serum creatinine and urinary creatinine concentrations were tested by an automated biochemical analyzer (Siemens biochemical analyzer and its Leadman reagent, Siemens, Germany). Urinary albumin concentrations were quantified using an enzyme-linked immunosorbent assay kit (ab235642, Abcam, Cambridge, UK). Urinary adenosine concentrations were determined by liquid chromatography-mass spectrometry (LC-MS/MS) as described previously(23). The concentration of empagliflozin in serum was measured using high performance liquid chromatography (HPLC) as previously described(21). Urinary albumin excretion rate (ACR), serum creatinine clearance (Ccr) and urinary adenosine excretion rate were calculated by equations: ACR (mg/g) = urinary albumin (mg/L) / urinary creatinine (umol/L); Ccr (ml/min) = [urinary creatinine (μmol/L) * urinary flow (ml/min)]/ serum creatinine (μmol/L); urinary adenosine excretion rate = urinary adenosine (umol/L) / urinary creatinine (umol/L).

2.3 Renal histological evaluation

After soaking in 4% paraformaldehyde for 48 hours, the kidneys were paraffin-embedded and placed at room temperature (25°C). Paraffin-embedded kidneys were made into 2μm thick sections for pathological staining analysis, including Periodic Acid-Schiff Stain (PAS), Sirius Red Stain, Periodic Schiff-Methylamine Stain (PASM) and Masson's Trichrome Stain (Masson). All stained slides were scanned panoramic at X400 pixels. iViewer 6.3.6 (UNIC TECHNOLOGIES, INC., China) was used to visualise and analyse these images. Glomerulosclerosis index, glomerular size, number of glomerular cells, renal interstitial fibrosis and perivascular fibrosis index were evaluated. Glomerular size and number of glomerular cells were assessed with iViewer 6.3.6 (UNIC TECHNOLOGIES, INC., China) on 50 randomly selected glomeruli per PASM-stained slide. Assessment of the glomerulosclerosis index was performed on PAS-stained slides. This assessment was performed by 2 researchers double-blinded to this experiment using a subjective semi-quantitative scoring system (score 1-4) to rate the percentage of PAS–positive areas within the glomerulus: 1=Slight, 2=Moderate, 3=Severe, 4=Highly severe. The perivascular fibrosis index was also assessed by 2 independent researchers on slides stained with Masson's trichrome using a semi-quantitative scoring system (score 1-4) as follows: 1=Slight, 2= Moderate, 3=Severe, 4=Highly severe. Analysis of renal interstitial fibrosis was performed by the ImageJ threshold method (National Institutes of Health, USA) measuring the percentage of fibrosis on images intercepted from Sirius Red-stained full-scan images at X400 pixels, as previously described(24). In all of the above analyses, the images being evaluated comprise more than 80% of each slide. All of the above semi-quantitative scoring analyses were analyzed by 2 independent researchers and the average of the two assessments was used for further analysis.

2.4 Immunofluorescence staining and analysis

Paraffin-embedded kidneys were made into 4μm thick sections for immunofluorescence analysis. First, the prepared frozen sections were immunofluorescently labelled with primary antibodies and placed at 4˚C overnight. Specific information on primary antibodies is as follows: anti-CD68 (GB113109, Servicebio, China, dilution 1:2000), anti-CD8 (GB11068, Servicebio, China, dilution 1:500) and anti-CD4 (GB11064- 1, Servicebio, China, dilution 1:500). Then the tissues and cells were washed and immunofluorescently labeled with secondary antibodies (anti-CD68. GB22303, Servicebio, China, dilution 1:500; anti-CD8 and anti-CD4: GB21303, Servicebio, China, dilution 1:300). Finally, the nuclei were stained with 4',6-diamidino-2-phenylindole (DAPI) and the tissues and cells were visualized. Twelve fields of view per slide were randomly intercepted under a fluorescence microscope at X200 pixels. Analysis of cytotoxic T cells (CD8+ cells/total cells) and helper T cells (CD4+ cells/total cells) was performed at Aipathwell (Servicebio, China), while the relative fluorescence units (RFU) of CD68 were assessed by ImageJ software (National Institutes of Health, USA). For all of the above analyses, images with the following were excluded: a) areas with non-specific staining patterns; b) areas with damaged or obscured tissue; c) areas outside our focus areas; d) areas with unclear nuclear staining; e) areas with unrelated tissue features, such as large blood vessels or large spaces.

2.5 RNA sequencing and quantitative real-time polymerase chain reaction

Based on the median of the final serum creatinine concentration, six kidney samples from each group that were soaked with RNA protective solution were selected for RNA sequencing analysis. The HiSeq 4000 platform device (Illumina, Inc; San Diego, CA, USA) was used for RNA sequencing analysis in which messenger RNA (mRNA) libraries were prepared, sequenced and data analysed as previously described(25). The 5/6Nx+placebo (PBO) group was used as a control group for comparison between groups, and genes with an absolute value of log2 (fold change) > 1 and a P value < 0.05 were considered differentially expressed genes (DEGs). The screened differential genes were ranked from lowest to highest P-value and six functional genes that were simultaneously up-/down-regulated in the control (5/6Nx+PBO and 5/6Nx+TELM) and intervention groups (5/6Nx+3mg EMPA and 5/6Nx+15mg EMPA) were selected for qRT-PCR validation (SDS7900HT; Thermo Fisher Scientific, Inc. Waltham, MA, USA). Ultimately, *C1QA* (complement component 1, Q subcomponent, A chain), *C1QC* (complement component 1, Q subcomponent, C chain), *FMOD* (fibronectin), *REN* (renin), *FMO2* (flavin-containing dimethylaniline monooxygenase 2) and *RPL36* (ribosomal protein L36) were validated by qRT-PCR, and these six genes were labelled in the volcano map. Six samples per group were selected for qRT-PCR validation. However, one sample from the 5/6Nx+15 mg Empagliflozin group had quality issues, resulting in only five data points for *C1QA, C1QC, FMOD, REN*, and *FMO2* in that group, while the other groups had six. To address this, we included an additional sample in the 5/6Nx+3 mg Empagliflozin, 5/6Nx+15 mg Empagliflozin, Sham+PBO and 5/6Nx+PBO groups during the final assay for *RPL36*.

2.6 Materials

Empagliflozin (EMPA) and telmisartan (TELM) were from Boehringer Ingelheim Pharma GmbH & Co. KG (Biberach an der Riss, Germany). Rats in the intervention groups were treated with empagliflozin/telmisartan dissolved in 0.5% w/v hydroxypropyl methylcellulose in water by gavage, whereas rats in sham group were treated with the corresponding volume of 0.5% w/v hydroxypropyl methylcellulose in water.

2.7 Statistical analysis

Data are showed as mean±SEM. Statistical analysis were conducted with GraphPad Prism 6 software (GraphPad, La Jolla, CA). The identification and exclusion of outliers was performed using ROUT (Q=1%) in the GraphPad Prism 6 software, which ultimately excluded only 2 outliers (1 from creatinine clearance in the 5/6Nx + TELM group and 1 from glomerular size in the 5/6Nx + PBO group). Two-way ANOVA followed by Bonferroni's post hoc test was applied to the simultaneous comparative analysis of serum creatinine concentrations between groups at multiple time points. For comparisons between groups, normally distributed data were analyzed using one-way ANOVA with Bonferroni's post hoc test, and non-normally distributed data were analyzed using Kruskal-Wallis test with Dunn's post hoc test. The Pearson correlation analysis was performed to assess correlation. In all cases, only $p<0.05$ was considered as a statistically significant difference.

3. Results

3.1 Effect of empagliflozin on renal function in 5/6 nephrectomized rats.

5/6 nephrectomy resulted in increased serum creatinine concentration, increased ACR, decreased Ccr, and prevented weight gain in rats (Table 1 and Figure 2). Telmisartan effectively alleviated severe albuminuria after renal injury, consistent with previous findings (Table 1 and Figure 2b). As shown in the baseline data in Table 1, the initial serum creatinine levels were higher in the 5/6Nx + 3 mg empagliflozin and 5/6Nx + 15 mg empagliflozin groups compared to the 5/6Nx + PBO group. We randomly assigned the animals to groups, and by chance, there were differences among them—a well-known phenomenon in pharmacological research. Even in the presence of unfavorable baseline variance factors, the final absolute values still demonstrated a significant reduction in serum creatinine in both the 5/6Nx + 3 mg and 5/6Nx + 15 mg empagliflozin groups compared to the 5/6Nx + PBO group. Furthermore, the relative change from baseline in serum creatinine also showed a significant reduction in the empagliflozin groups. Serum creatinine clearance followed a similar pattern. These findings suggest that the actual renoprotective effect of empagliflozin is likely more pronounced than indicated by the data alone. 5/6Nx-mediated renal injury was significantly improved by high-dose empagliflozin treatment, such as decreased serum creatinine concentration, decreased ACR, and increased Ccr (Table 1 and Figure 2). According to the current data, the reno-protective effect of empagliflozin was superior to that of the current gold standard angiotensin II receptor blocker, telmisartan. In addition, empagliflozin-mediated renal protection showed a dose-dependent effect. Low-dose empagliflozin treatment only reduced serum creatinine levels in 5/6Nx rats (Table 1 and Figure 2). Relative kidney weights were not statistically different between groups (Table 1). Urine albumin concentrations were measured only at the end of the experiment, so only the final ACR is presented. Due to disease and operations resulting in the loss of some animals, the final number of animals in each group was as follows: Sham + Placebo (7 animals), 5/6Nx + Placebo (9 animals), 5/6Nx + 3 mg Empagliflozin (9 animals), 5/6Nx + 15 mg Empagliflozin (11 animals), and 5/6Nx + Telmisartan (7 animals). After excluding deaths unrelated to the disease, the mortality rate for each group was: Sham + Placebo (12.50%), 5/6Nx + Placebo (40.00%), 5/6Nx + 3 mg Empagliflozin (30.77%), 5/6Nx + 15 mg Empagliflozin (21.43%), and 5/6Nx + Telmisartan (30.0%). Mortality analyses showed no significant differences between groups, so these data are not presented graphically.

Table 1: Animal characteristics.

Parameters	Sham+PBO (n=7-10)	5/6Nx+PBO (n=9-15)	5/6Nx+3mg EMPA (n=9-15)	5/6Nx+15mg EMPA (n=11-15)	5/6Nx+TELM (n=7-15)
			Baseline		
Body weight (g)	298.50±5.23	315.79±6.46	350.38±8.31*	333.00±10.06	349.00±9.79
Serum creatinine (µmol/L)	18.50±1.50	18.00±1.44	25.85±1.25**	26.86±1.29***	22.22±1.78
Ccr (ml/min)	2.01±0.28	1.98±0.14	1.72±0.17	1.34±0.11*	1.76±0.27
			Final value		
Body weight (g)	509.00±18.09	464.11±17.58	494.56±16.37	468.18±13.11	475.29±11.36
Kidney weight (g)	2.07±0.11	2.34±0.18	2.69±0.27	2.85±0.12	1.95±0.14
Rel. kidney weight (10^{-2})	0.41±0.02	0.51±0.06	0.55±0.05	0.61±0.03	0.41±0.03
Serum creatinine (µmol/L)	24.00±1.51****	72.00±8.49	47.50±4.98**	49.09±2.76**	54.86±2.42
Ccr (ml/min)	2.82±0.24****	1.14±0.14	1.69±0.21	1.90±0.15**	1.12±0.08
ACR (mg/g*10^{-2})	6.66±3.83*	61.75±28.79	24.28±7.85	8.48±1.70*	6.88±3.10*
T_{24} (Empagliflozin, nM)	-	-	-	23.20 ± 6.50	-
			Change from baseline		
Body weight (g)	208.57±20.75*	149.11±11.60	149.56±17.53	146.36±7.23	139.71±15.05
Serum creatinine (µmol/L)	5.71±0.81****	53.78±8.85	23.00±4.94***	22.91±2.29***	37.14±3.46
Ccr (ml/min)	0.86±0.28***	-0.99±0.27	-0.11±0.21	0.56±0.18**	-0.50±0.29

Body weight (change from baseline) = Final body weight – Baseline body weight; Rel. kidney weight (Relative kidney weight) = kidney weight / final body weight; ACR (urinary albumin to creatinine ratio) = urinary albumin / urine creatinine; Ccr (creatinine clearance) = [urinary creatinine (µmol/L) * urinary flow (ml/min)]/ serum creatinine (µmol/L); Ccr (change from baseline) = Final Ccr – Baseline Ccr; Sham: Sham operation; 5/6Nx: 5/6 nephrectomized rat model; PBO: Placebo; TELM: Telmisartan; EMPA: Empagliflozin. T24 (Empagliflozin, nM): Plasma concentrations of empagliflozin after 24 hours of gavage. -: Below the minimum detection value. Values displayed are mean ± SEM. *p<0.05; **p<0.01; ***p<0.001; ****p<0.0001, significantly different from 5/6Nx + PBO. Citation: This table has been modified from that in the paper - Chen, et al. 2023(22). Baseline and final data have been added to the table.

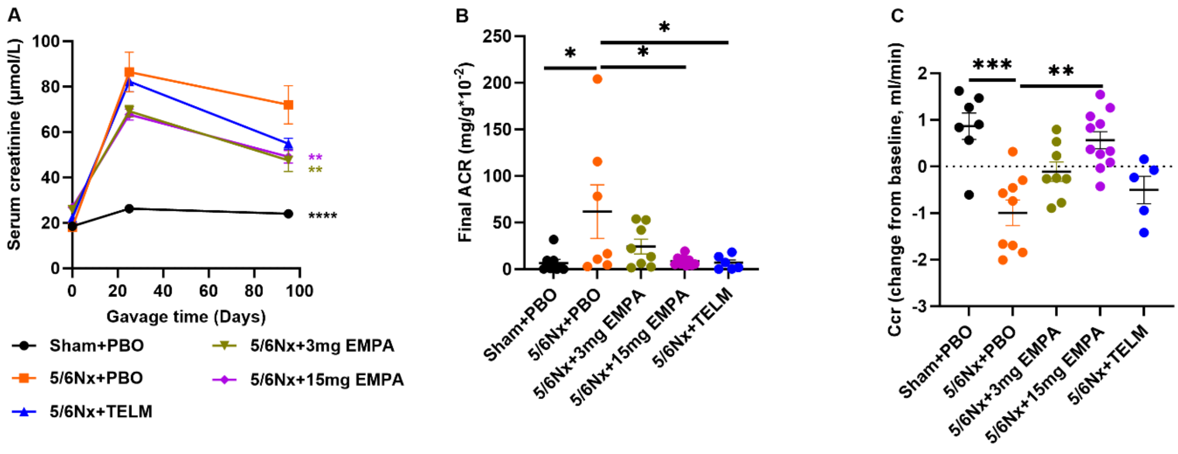

Figure 2: Effects of empagliflozin on renal function in 5/6 nephrectomized rats. (A) Serum creatinine concentration in the research process: The serum creatinine of rats in group 5/6Nx + PBO was higher than sham + PBO, 5/6Nx + 3mg EMPA and 5/6Nx + 15mg EMPA; (B) Final ACR: Sham + PBO, 5/6Nx + 15mg EMPA and 5/6Nx + TELM were lower than 5/6Nx + PBO; (C) Ccr (change from baseline): Ccr in 5/6Nx + PBO group was lower than in sham + PBO and 5/6Nx + 15mg EMPA groups. Sham: Sham operation; 5/6Nx: 5/6 nephrectomized rat model; PBO: Placebo; TELM: Telmisartan; EMPA: Empagliflozin. ACR: urinary albumin to creatinine ratio; Ccr: Serum creatinine clearance. Values shown are means ± SEM. *$p<0.05$; **$p<0.01$; ***$p<0.001$; ****$p<0.0001$, significantly different from 5/6Nx + PBO. Citation: This figure has been modified from that in the paper - Chen, et al. 2023(22). The horizontal axis in Figure 2A has been revised from displaying months to displaying days.

3.2 Effect of empagliflozin on renal histopathology in 5/6 nephrectomized rats.

Compared to the Sham+PBO group, 5/6 nephrectomy resulted in severe fibrosis, including renal interstitial fibrosis, perivascular fibrosis, and glomerulosclerosis, as well as increased number of glomerular cells and glomerular size (Figure 3 A-F). All of the above morphological parameters improved with both 3mg and 15mg doses of empagliflozin treatment (Figure 3 A-F). Both 3mg and 15mg doses of empagliflozin treatment substantially reduced the severity of renal interstitial fibrosis, perivascular fibrosis and glomerulosclerosis. The effect on glomerular size was relatively less pronounced but showed a dose-dependent effect consistent with the effect on functional parameters (Figure 3F). The angiotensin II receptor blocker telmisartan, consistent with many previous studies, significantly improved renal fibrosis (Figure 3A-F).

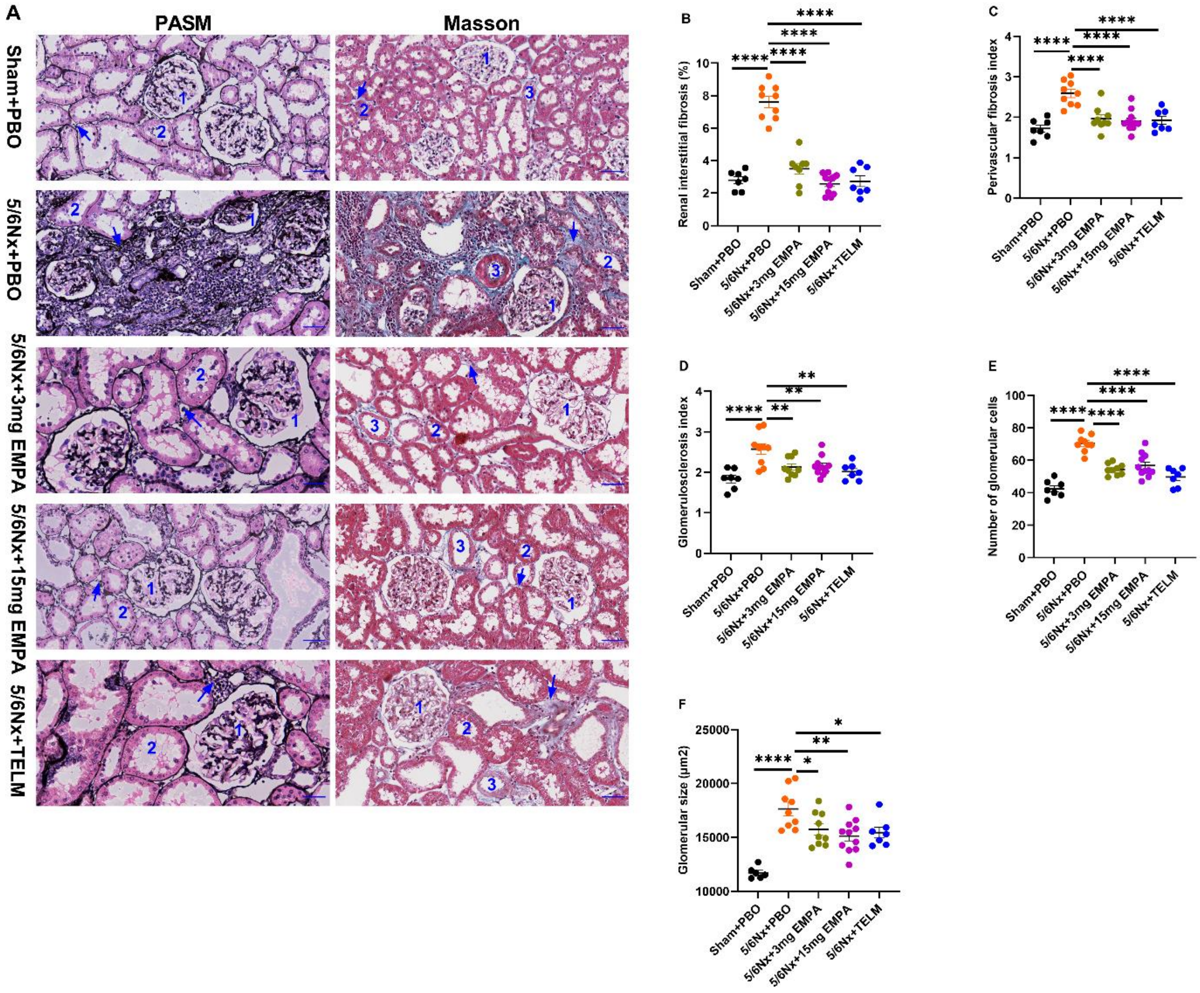

Figure 3: Histopathological effects of empagliflozin on 5/6 nephrectomized rats. (A) Representative micrographs of PASM and Masson staining of kidney tissue from all groups (X400, Scale bar=50μm); Label 1: Glomerulus; Label 2: Renal tubules; Label 3: Vascular; Arrow: Renal interstitial fibrosis. (B) Renal interstitial fibrosis (%); (C) Perivascular fibrosis index; (D) Glomerulosclerosis index; (E) Number of glomerular cells; (F) Glomerular size (μm2). All these indicators were lower in the other groups than in the 5/6Nx + PBO group. Sham: Sham operation; 5/6Nx: 5/6 nephrectomized rat model; PBO: Placebo; TELM: Telmisartan; EMPA: Empagliflozin. Values displayed are means ± SEM. *p<0.05; **p<0.01; ***p<0.001; ****p<0.0001, significantly different from 5/6Nx + PBO. Citation: This figure is quoted from the paper - Chen, et al. 2023(22).

3.3 Effect of empagliflozin on urinary adenosine excretion in 5/6 nephrectomized rats.

5/6 Nephrectomy resulting in severely reduced urinary adenosine excretion (Figure 4A). Empagliflozin treatment corrected the decrease in urinary adenosine excretion rate induced by 5/6Nx (Figure 4A). However, the effect of empagliflozin on urinary adenosine was only seen in the high dose group. Even though the urinary adenosine excretion rate was elevated in the low-dose group compared to the 5/6Nx+PBO group, there was no statistical difference. The telmisartan-treated group also showed a trend of increased urinary adenosine excretion rate, but there was no statistical difference (p=0.057, Figure 4A). The urinary adenosine excretion rate in rats correlated with morphological parameters of the kidney and serum creatinine clearance (Figure 4B-D). Urinary adenosine excretion rate was negatively associated with the degree of renal interstitial fibrosis (Figure 4B) and glomerular size (Figure 4C), and positively associated with Ccr (Figure 4D).

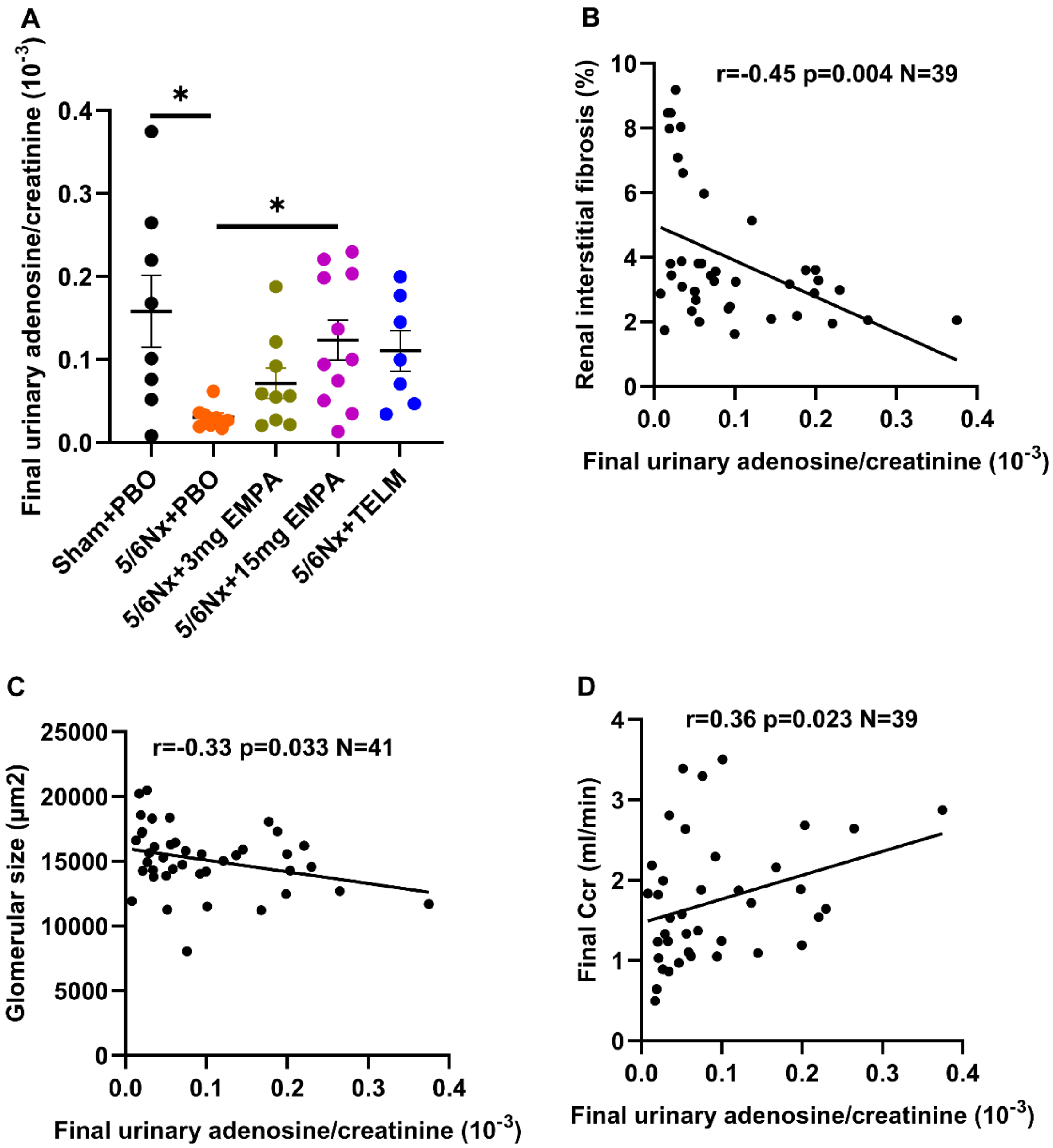

Figure 4: Effect of empagliflozin on final urinary adenosine/creatinine ratio in 5/6 nephrectomised rats and correlation of final urinary adenosine/creatinine ratio with histological parameters. (A) Comparison of final urinary adenosine excretion rates between treatment groups and 5/6Nx+PBO: final urinary adenosine/creatinine in group 5/6Nx + PBO was lower than in sham + PBO and 5/6Nx + 15mg EMPA groups. Sham: Sham operation; 5/6Nx: 5/6 nephrectomized rat model; PBO: Placebo; TELM: Telmisartan; EMPA: Empagliflozin. Values displayed are means ± SEM. *$p<0.05$, significantly different from 5/6Nx + PBO. (B) Correlation of the final urinary adenosine/creatinine ratio with renal interstitial fibrosis: At the end of the study, the urinary adenosine/creatinine ratio was inversely correlated with renal interstitial fibrosis (r=-0.45 p=0.004 N=39). (C) Correlation of the final urinary adenosine/creatinine ratio with glomerular size: At the end of the study, the urinary

adenosine/creatinine ratio was negatively correlated with glomerular size (r=-0.33 p=0.033 N=41). (D) Correlation of the final urinary adenosine/creatinine ratio with Ccr: At the end of the study, the urinary adenosine/creatinine ratio was positively correlated with Ccr (r=0.36 p=0.023 N=39). Ccr: Serum creatinine clearance. Citation: This figure is quoted from the paper - Chen, et al. 2023(22).

3.4 Effect of empagliflozin on macrophages and T cells in 5/6 nephrectomized rats.

The densities of cytotoxic T cells (CD8+ cells/total cells) and helper T cells (CD4+ cells/total cells) in the kidney were not statistically different between 5/6Nx + PBO, sham+PBO and treatment groups (Figure 5 A-C). Renal CD68+ cell (macrophage) infiltration was enhanced in the 5/6Nx+PBO group compared with Sham+PBO (P=0.047), whereas neither empagliflozin nor telmisartan treatment had any effect on the 5/6 nephrectomy-mediated increase in macrophage infiltration (Figures 5A and D).

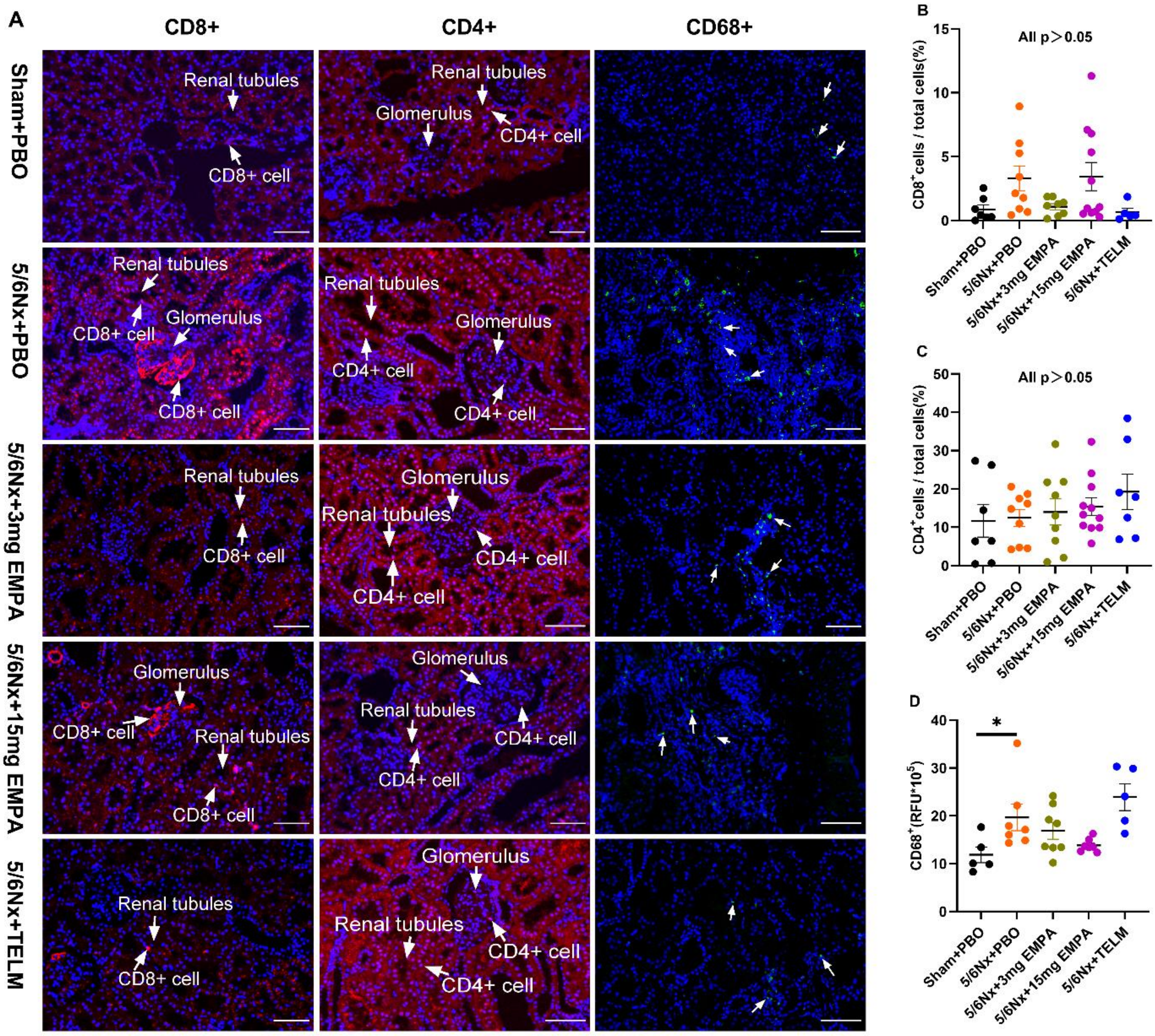

Figure 5: Immunofluorescence staining analysis of T cells and macrophages in kidney tissues. (A) Representative micrographs of kidney tissues from all treatment groups (X200, Scale bar=100μm); (B) Cytotoxic T cells (CD8+cells/total cells, %): no statistical difference between groups; (C) Helper T cells (CD4+cells/total cells, %): no statistical difference between groups; (D) Macrophages (CD68+, RFU): 5/6Nx + PBO was higher than Sham + PBO group. The arrows point to CD68+ cells. RFU: Relative fluorescence unit. Sham: Sham operation; 5/6Nx: 5/6 nephrectomized rat model; PBO: Placebo; TELM: Telmisartan; EMPA: Empagliflozin. Values displayed are means ± SEM. *p<0.05, significantly different from 5/6Nx + PBO. Citation: This figure is quoted from the paper - Chen, et al. 2023(22).

3.5 Effect of empagliflozin on complement system in 5/6 nephrectomized rats.

The differentially expressed genes screened from the RNA sequencing data according to the methodology described above are presented in the Venn diagram (Figure 6A and

Figure 7A), from which it can be seen that there are 4 co-regulated differentially expressed genes between the 5/6Nx + 3mg EMPA, 5/6Nx + 15mg EMPA, and 5/6Nx + PBO groups. There were 73 co-regulated differentially expressed genes between the 5/6Nx + 3mg EMPA and 5/6Nx + PBO groups, and 11 co-regulated differentially expressed genes between the 5/6Nx + 15mg EMPA and 5/6Nx + PBO groups. From these co-regulated differentially expressed genes, six functional genes were selected for qRT-PCR validation, as described in the Methods section. Ultimately, six genes, *C1QA*, *C1QC*, *FMOD*, *REN*, *FMO2* and *RPL36*, were validated (Figure 7). Only *C1QA* and *C1QC* genes showed a model effect - being upregulated after 5/6 nephrectomy and responding to empagliflozin treatment (Figure 7B and C). 5/6 Nephrectomy did not significantly alter *REN* expression; however, the angiotensin II receptor blocker telmisartan substantially upregulated *REN* expression, which is well known to be the effect of telmisartan.

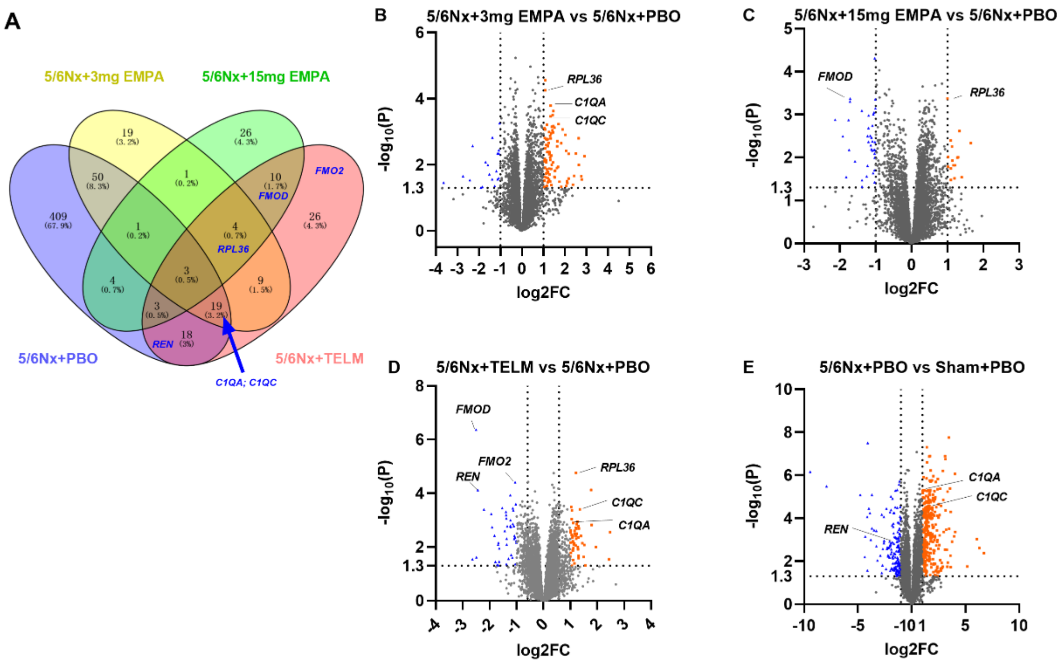

Figure 6: Differentially expressed genes in kidney tissue detected by RNA sequencing. (A) Venn diagram showing differentially expressed genes in the 5/6Nx + PBO, 5/6Nx + TELM, 5/6Nx + 3mg EMPA and 5/6Nx + 15mg EMPA groups. Circles represent the total number of statistically significant (p value < 0.05 and an absolute value of log2(fold change) > 1) differentially expressed genes detected by RNA sequencing in the 5/6 Nx + 3mg EMPA, 5/6 Nx + 15mg EMPA and 5/6 Nx + TELM groups compared to 5/6 Nx + PBO. (B) Volcano plot of RNA-sequencing data showing gene expression values in 5/6Nx + 3mg EMPA group relative to the 5/6Nx+PBO group. (C) Volcano plot of RNA-sequencing data showing gene expression values in 5/6Nx + 15mg EMPA

group relative to the 5/6Nx+PBO group. (D) Volcano plot of RNA-sequencing data showing gene expression values in 5/6Nx + TELM group relative to the 5/6Nx+PBO group. (E) Volcano plot of RNA-sequencing data showing gene expression values in Sham + PBO group relative to the 5/6Nx+PBO group. Genes are color-marked if they pass the threshold of p=0.05 and log2 (fold change) = ±1, with up-regulated genes marked in orange and down-regulated genes marked in blue. The functional differentially expressed genes that were screened for qRT-PCR confirmation were labeled. Sham: Sham operation; 5/6Nx: 5/6 nephrectomized rat model; PBO: Placebo; TELM: Telmisartan; EMPA: Empagliflozin; qRT-PCR: Quantitative Reverse Transcription Polymerase Chain Reaction; *C1QA*: Complement Component 1, Q Subcomponent, A Chain; *C1QC*: Complement Component 1, Q Subcomponent, C Chain; *FMOD*: Fibromodulin; *REN*: Renin; *FMO2*: Flavin Containing Dimethylaniline Monoxygenase 2; *RPL36*: Ribosomal Protein L36. Citation: This figure is quoted from the paper - Chen, et al. 2023(22).

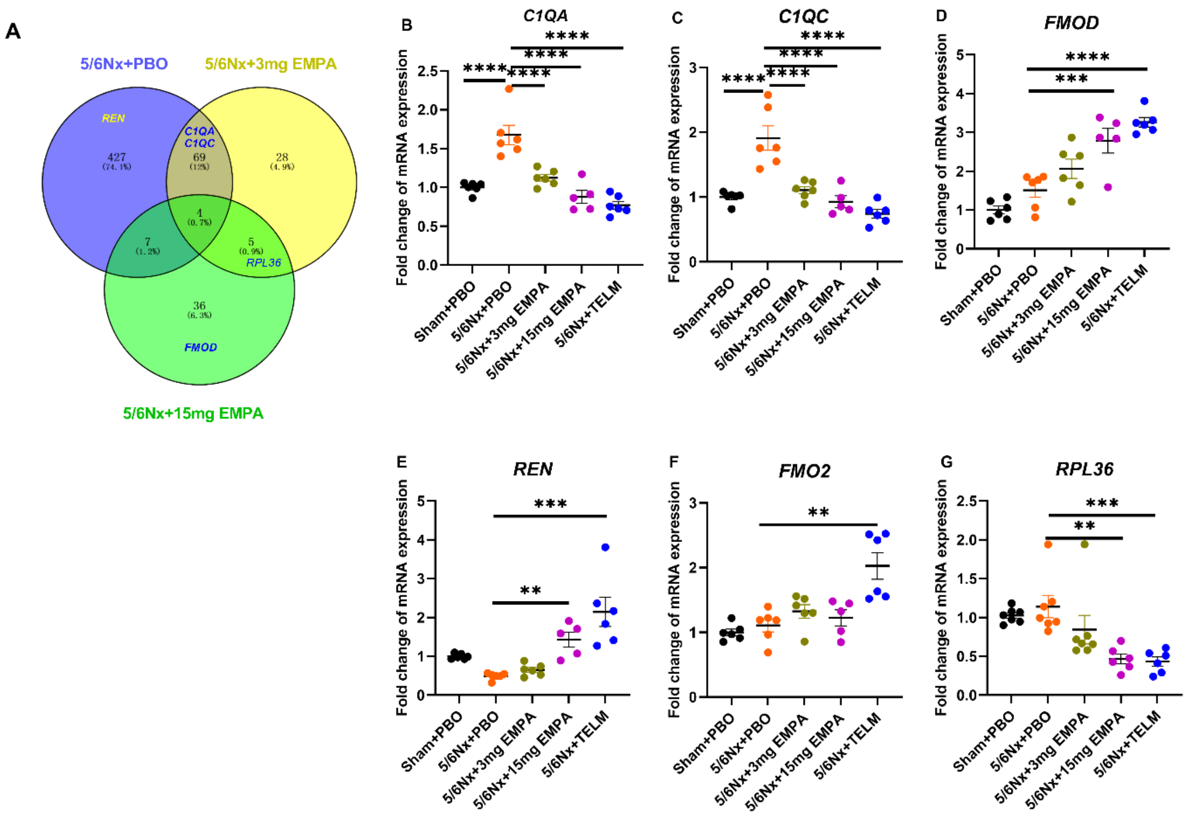

Figure 7: Gene expression in the kidney identified by qRT-PCR. (A) Venn diagram showing differentially expressed genes in the 5/6Nx + PBO, 5/6Nx + 3mg EMPA and 5/6Nx + 15mg EMPA groups. Circles represent the total number of differentially expressed genes in the 5/6 Nx + 3mg EMPA and 5/6 Nx + 15mg EMPA that were statistically significant (p value < 0.05 and an absolute value of log2(fold change) > 1) compared to the 5/6 Nx + PBO group as detected by RNA-sequencing. (B) Fold change of *C1QA* expression: Complement Component 1, Q Subcomponent,

A Chain; (C) Fold change of *C1QC* expression: Complement Component 1, Q Subcomponent, C Chain; (D) Fold change of *FMOD* expression: Fibromodulin; (E) Fold change of *REN* expression: Renin; (F) Fold change of *FMO2* expression: Flavin Containing Dimethylaniline Monoxygenase 2; (G) Fold change of *RPL36* expression: Ribosomal Protein L36. Sham: Sham operation; 5/6Nx: 5/6 nephrectomized rat model; PBO: Placebo; TELM: Telmisartan; EMPA: Empagliflozin; qRT-PCR: Quantitative Reverse Transcription Polymerase Chain Reaction. Values displayed are means ± SEM. **p<0.01; ***p<0.001; ****p<0.0001, significantly different from 5/6Nx + PBO. Citation: This figure is quoted from the paper - Chen, et al. 2023(22).

4. Discussion

4.1 Summary of results.

This study in a classical CKD rat model (5/6 nephrectomy) revealed dose-dependent reno-protective effects of the SGLT2 inhibitor empagliflozin independent of glycemic control, including a dose-dependent preventing of the decrease in serum creatinine clearance, a dose-dependent reduction in urinary protein excretion rate and improvement in renal interstitial fibrosis and glomerulosclerosis. These reno-protective effects of empagliflozin were accompanied by a dose-dependent effect on the urinary adenosine excretion rate - a surrogate parameter of the TGF mechanism. Furthermore, in this study, we revealed for the first time that activation of the TGF mechanism is negatively related to renal interstitial fibrosis and glomerular size and positively related to Ccr. In addition, RNA sequencing and subsequent qRT-PCR confirmation provided for the first time that empagliflozin alters the expression of key genes of the complement system, which is a key mechanism of kidney injury.

4.2 Comparison with current studies.

This study is consistent with all the large clinical trials with and without diabetic kidney disease mentioned in the introductory section in supporting that SGLT2 inhibitors improve renal function in CKD. Several animal studies have provided evidence for the reno-protective effects of SGLT2 inhibitors, but inadequately, most of the animal experiments have been performed in diabetic nephropathy models, whereas the few studies performed in non-diabetic nephropathy models have shown contradictory findings. Our findings are in agreement with those of di Gioia, C. R. T.(18) and Awad, M. M.(26) et al. showing the nephroprotective effect of SGLT2 inhibitors. However, studies by Gilbert, R. E.(dapagliflozin 0.5 mg/kg, twice/day, 12 weeks)(19), Advani A (dapagliflozin 1mg/kg/d for 8 weeks)(27), Anders, H. J.(empagliflozin 10mg/kg/d for 7 or 14 days)(28) et al. contradict showing no effect of SGLT2 inhibition on non-diabetic CKD models. CKD is a chronic progressive deteriorating disease and therefore the timing as well as the duration of pharmacological intervention are important for renal prognosis. Some studies therapeutic duration of less than 6 weeks did not find evidence of a reno-protective effect of SGLT2 inhibitors(28), whereas in our study we treated the CKD rats for more than 13 weeks. Thus, one reason for differences among published studies might be the treatment duration of SGLT2 inhibitors. In addition to the treatment duration factor, medication dose is another key factor influencing the medication effect, as our study shows the dose dependence of the nephroprotective effect of SGLT2 inhibitors - serum creatinine clearance and urinary protein excretion rates were improved in rats only under empagliflozin (15 mg/kg/d) treatment. Advani A and Cherney DZI. et al. used dapagliflozin (1 mg/kg/d) for 8 weeks in a 5/6 nephrectomy model but found no evidence of renal benefit from dapagliflozin(27). Although the study by Gilbert, R. E. et al.(19) was also performed in a 5/6 nephrectomy rat model and the duration of treatment was almost the same as in our study, the dose of dapagliflozin (0.5 mg/kg, twice/day) used was much lower than in our study, which may explain the non-significant reno-protective effect observed in some experiments. Further, although the major current SGLT2 inhibitors, such as canagliflozin, empagliflozin, and dapagliflozin, all act primarily on SGLT2 in the proximal tubules of the kidney, they differ in their chemical structural formula and pharmacokinetics(29). In addition, SGLT2 inhibitors are likely involved in adenosine-mediated TGF regulation by affecting urinary sodium concentration, so other factors should be avoided when exploring the reno-protective effects of SGLT2 inhibitors, as Tauber et al.(30) using an adenosine-induced CKD model and Vervaet et al.(31) using a unilateral nephrectomy CKD model under a high salt diet, neither found positive renal effects of SGLT2 inhibitors. However, in clinical applications, SGLT2 inhibitors appear to prevent the progression of chronic kidney disease due to any type of primary disease.

4.3 Empagliflozin mediates nephroprotection by activation of TGF.

TGF is a key mechanism by which the kidney maintains stable intra-glomerular pressure and glomerular filtration rate. The presence of TGF optimizes the oxygenation-perfusion matching of the renal vascular unit. Focal segmental glomerulosclerosis and its corresponding TGF inactivation are common in CKD, and these lesions cause increased filtration pressure and abnormal TGF response in the residual renal unit. Prolonged elevated intra-glomerular pressure and hyperfiltration disrupt normal renal histology and induce inflammation and fibrosis, so restoring regulation of impaired TGF is likely to prevent deterioration of the remnant renal unit. Physiologically, the macula densa of the thick ascending branch of the renal tubular cortex senses changes in urinary sodium concentration and adjusts the tension of the glomerular afferent arteriole via adenosine-mediated signaling feedback(2). Theoretically, SGLT2 inhibitors block sodium-glucose cotransport in the renal tubules leading to an increase in sodium concentration flowing through the macula densa, which in turn promotes the degradation of adenosine triphosphate (ATP) to adenosine in the macula densa. Adenosine acts on adenosine receptors (G-protein-coupled receptors) on vascular smooth muscle cells to constrict glomerular afferent arterioles, thereby reducing glomerular blood perfusion and lowering intra-glomerular pressure. Renin-angiotensin-aldosterone system (RAAS) blockers are widely used in the treatment of CKD precisely because they can protect the kidney by lowering intra-glomerular pressure as well. In fact, several studies have now provided evidence that SGLT2 inhibitors regulate TGF(32) including our current study. Urinary adenosine excretion rate is a reliable indirect method for monitoring the effect of medication on TGF(2), and this method was also applied to our present study. At the end of the research, we examined the urinary adenosine excretion rate of rats in each group. We found that the urinary adenosine excretion rate decreased after 5/6Nx and was restored after empagliflozin treatment. In other words, empagliflozin corrected the abnormal regulation of TGF after renal injury, thereby reducing intra-glomerular pressure and protecting the kidneys. Our study clearly links renal protection by SGLT2 inhibitors to urinary adenosine excretion in a classical non-diabetic CKD model. More importantly, the association between Ccr, renal interstitial fibrosis, glomerular size and urinary adenosine excretion rate at the end of the study shows for the first time a relationship between the functional and histological characteristics of CKD and urinary adenosine excretion rate, a surrogate parameter for TGF activity. Activation of TGF was beneficial in reducing interstitial fibrosis and improving serum creatinine clearance (Figure 4). However, this finding is inconsistent with the results of our earlier study on TGF, which concluded that empagliflozin had no effect on urinary adenosine excretion rates in 5/6 nephrectomized rats on a high-salt diet(21). Both studies used a 5/6 nephrectomized animal model and the same analytical techniques to study the effects of empagliflozin, but the only key difference was the level of salt in the diet. Changes in urinary sodium concentration are a key component of TGF regulation and a bridge for SGLT2 inhibitors to regulate TGF. Under a high-salt diet, urinary sodium concentration persists at high levels, which covers the regulation of urinary sodium concentration by SGLT2 inhibitors. Therefore, we infer that empagliflozin-mediated renoprotection under high salt diet conditions appears to be independent of TGF, which appears to play a key role under normal salt intake. Further investigation of the effects of SGLT2 inhibitors in a TGF-deficient animal model (adenosine-1 receptor knockout mice) would be beneficial to verify the relationship. Furthermore, decreased glomerular filtration rate was observed in some animal models(31), but not in our study. We suggest that this is related to the timing of the medication intervention, as shown in a large controlled clinical trial in which a transient and dramatic decrease in glomerular filtration rate occurred within 2 months of SGLT2 inhibitor treatment, while the subsequent decrease in glomerular filtration rate slowed significantly relative to control group(16). Thus, we suggest that empagliflozin may have a long-term reno-protective effect through other mechanisms beyond the effects on the TGF.

4.4 Effect of empagliflozin on renal inflammation and fibrosis.

A study by Kim, G. H. et al.(33) and one of our recently published studies (34) have shown that SGLT2 inhibitors ameliorate renal fibrosis in CKD rats by inhibiting macrophage differentiation, diminishing T-cell infiltration and the expression of inflammatory factors. We believe that this is related to the timing of sample collection. The pathological changes in the early stages of kidney injury are dominated by inflammatory infiltrates and transition to fibrosis as the disease progresses. Our current study similarly showed that SGLT2 inhibitors attenuated interstitial fibrosis and glomerulosclerosis in the kidneys of CKD rats. However, we did not find an effect of SGLT2 inhibitors on macrophages and T cells. In our study, the duration of treatment beyond 13 weeks was longer than in most other experiments. In advanced stages, inflammation may no longer be the primary pathophysiology. A study that ended the experiment 8 weeks after renal injury similarly found no evidence that SGLT2 inhibitors affected macrophages(27). In addition, the method used to investigate the effect of empagliflozin on inflammatory cells is also an influencing factor. In our earlier published study, we only used single-cell RNA sequencing in one animal subpopulation due to budgetary constraints and did not confirm the findings by a second independent technique(34). Further, in our previous study we only observed differences in macrophage subtype expression and did not analyze overall macrophage density. Therefore, we used a more sensitive technique in this study, whereby immunofluorescence staining was performed on all animals to detect the number of CD4+ and CD8+ cells, as well as the relative fluorescence units (RFU) of CD68+ cells in the kidney. No statistically significant differences were found between groups for CD4+ and CD8+ T cells and CD68+ cells (Figure 5), which is in line with the results of another study performed on a non-diabetic CKD rat model(27). The effects of SGLT2 inhibitors on T cells and macrophages are still not clearly described by the present findings. Multiple sampling of experimental animals at different time points in a long-term study would be beneficial in understanding the effects of SGLT2 inhibitors at different stages of CKD. More precisely, the possibility that macrophage polarization plays a pathophysiological role in the early stages of kidney injury cannot be excluded on the basis of our current study.

Based on the complexity of the SGLT2 inhibitor mechanism, we used in addition a non-hypothesis-driven approach - a strategy of whole genome RNA sequencing followed by qRT-PCR validation. This analysis revealed that upregulation of complement system components *C1QA* and *C1QC* due to 5/6 nephrectomy was corrected by empagliflozin in a dose-dependent way (Figures 6 and 7). *C1QA* and *C1QC* belong to the first component of complement, *C1Q* (subcomponent of complement component 1Q), which plays a highly critical role in innate and adaptive immune responses. Some evidence suggests that complement is a key mediator of renal interstitial fibrosis. Proximal tubular epithelial cells, glomerular epithelial cells and mesangial cells produce complement and activate complement cascade reactions in response to damage-associated molecular patterns (DAMPs), thereby promoting inflammatory responses(35). *C1QA* and *C1QC* are key factors in the classical pathway of complement activation. Activation of the complement cascade reaction produces anaphylatoxins (C3a, C5a and C5b). These anaphylatoxins are not only involved in the activation of the cytosolic inflammasome (NLRP3) but also in renal fibrosis, such as stimulating the secretion of transforming growth factor β1 (TGF-β1) from renal tubular epithelial cells to mediate renal fibrosis, activating fibroblasts and inducing transdifferentiation of pericytes to myofibroblasts(35). In addition, these anaphylatoxins stimulate the secretion of TGF-β and platelet-derived growth factor (PDGF) by endothelial cells, monocytes, and renal tubular epithelial cells, further activating fibroblasts to promote collagen deposition(36). Uncontrolled complement activation eventually leads to irreversible fibrosis in the kidney. There are now evidences that inhibition of complement activation ameliorates renal fibrosis. A study of a renal IRI injury model revealed that C1 esterase inhibitors reduced infiltration of inflammatory cells and reduced endothelial-to-mesenchymal (EndMT) transition and renal fibrosis(37). Delpech et al. also demonstrated that C1 esterase inhibitors reduced chronic fibrosis in renal transplants(38). Empagliflozin likely also blunted the complement system by inhibiting *C1QA* and *C1QC*, thereby reducing inflammation and fibrosis in the kidney.

4.5 Strengths and limitations of the study and implications for future research

A classical non-diabetic CKD nephropathy model was applied to explore other nephroprotective mechanisms of SGLT2 inhibitors beyond glycemic control. Two empagliflozin treatment doses were set to explore the possible potential dose-dependent effects of SGLT2 inhibitors. We found that SGLT2 inhibitors dose-dependently improved renal function in CKD. Furthermore, we demonstrated that empagliflozin corrected TGF abnormalities in CKD and showed for the first time a correlation between urinary adenosine excretion rate, a surrogate for TGF, and renal histopathological parameters. This study not only investigated the prespecified mechanisms, but also explored potential unknown mechanisms of SGLT2 inhibitors using whole genome RNA sequencing and qRT-PCR revalidation techniques. We present for the first time the effect of SGLT2 inhibitors on the C1 component of the complement system. However, our study still has some limitations. CKD is a progressive deteriorating disease, and we only performed pathological assessment and gene expression analysis at the end of the experiment, so we were unable to analyze the effect of SGLT2 inhibitors on different stages of CKD. Some clinical trials have shown that the effect of SGLT2 inhibitors on GFR varies over time, so the response of TGF to SGLT2 inhibitors may reset over time, but we only measured urinary adenosine concentrations in rats at the end of the experiment. Our experiments suggest two mechanisms of renal protection for empagliflozin - TGF-mediated action and altered gene expression of key components of the complement system. However, we did not validate their causal relationship in knockout animal models or cellular experiments. Second, since the effects of oral drugs are systemic and SGLT2 has been shown to be expressed in multiple organs of the body, it is possible that SGLT2 inhibitors may also benefit the kidney by acting on other systems, but we only analyzed kidney. Lastly, we focused on the pure effects of SGLT2 inhibitor therapy in this study, and the combination of SGLT2 inhibitors with the current gold standard of treatment, angiotensin receptor blockers, would also have pharmacological and pathophysiological implications.

5. Conclusions

This study provides evidence for the reno-protective effects of empagliflozin in non-diabetic CKD, including improvements in proteinuria, Ccr, glomerulosclerosis, renal interstitial fibrosis, and renal perivascular fibrosis. Furthermore, we show for the first time that urinary adenosine excretion rate, a surrogate indicator of TGF activity, correlates with renal functional and structural parameters. We infer that the reno-protective effect of empagliflozin is likely mediated by restoring TGF abnormalities after renal injury. In particular, these effects of empagliflozin were more pronounced in the high-dose empagliflozin (15 mg/kg/d) treatment group, suggesting that the reno-protective effects of SGLT2 inhibitors are likely to be dose-dependent. In addition to the TGF effect, genome-wide RNA sequencing and qRT-PCR of differentially expressed genes showed that empagliflozin limited complement cascade-mediated renal inflammation and fibrosis in non-diabetic CKD by down-regulating complement components C1QA and C1QC expression, thereby improving the structure and function of CKD.

References

1. Webster AC, Nagler EV, Morton RL, Masson P. Chronic Kidney Disease. Lancet. 2017;389(10075):1238-52.

2. Castrop H. Mediators of tubuloglomerular feedback regulation of glomerular filtration: ATP and adenosine. Acta Physiol (Oxf). 2007;189(1):3-14.

3. Lim BJ, Yang JW, Zou J, Zhong J, Matsusaka T, Pastan I, Zhang MZ, Harris RC, Yang HC, Fogo AB. Tubulointerstitial fibrosis can sensitize the kidney to subsequent glomerular injury. Kidney Int. 2017;92(6):1395-403.

4. Kriz W, Lemley KV. A potential role for mechanical forces in the detachment of podocytes and the progression of CKD. J Am Soc Nephrol. 2015;26(2):258-69.

5. Chen JK, Nagai K, Chen J, Plieth D, Hino M, Xu J, Sha F, Ikizler TA, Quarles CC, Threadgill DW, Neilson EG, Harris RC. Phosphatidylinositol 3-kinase signaling determines kidney size. J Clin Invest. 2015;125(6):2429-44.

6. Vallon V, Thomson SC. Renal function in diabetic disease models: the tubular system in the pathophysiology of the diabetic kidney. Annu Rev Physiol. 2012;74:351-75.

7. Anders HJ, Schaefer L. Beyond tissue injury-damage-associated molecular patterns, toll-like receptors, and inflammasomes also drive regeneration and fibrosis. J Am Soc Nephrol. 2014;25(7):1387-400.

8. Portilla D, Xavier S. Role of intracellular complement activation in kidney fibrosis. Br J Pharmacol. 2021;178(14):2880-91.

9. Huen SC, Cantley LG. Macrophages in Renal Injury and Repair. Annu Rev Physiol. 2017;79:449-69.

10. Liu L, Kou P, Zeng Q, Pei G, Li Y, Liang H, Xu G, Chen S. CD4+ T Lymphocytes, especially Th2 cells, contribute to the progress of renal fibrosis. Am J Nephrol. 2012;36(4):386-96.

11. Dong Y, Yang M, Zhang J, Peng X, Cheng J, Cui T, Du J. Depletion of CD8+ T Cells Exacerbates CD4+ T Cell-Induced Monocyte-to-Fibroblast Transition in Renal Fibrosis. J Immunol. 2016;196(4):1874-81.

12. Nespoux J, Vallon V. SGLT2 inhibition and kidney protection. Clin Sci (Lond). 2018;132(12):1329-39.

13. Wanner C, Inzucchi SE, Lachin JM, Fitchett D, von Eynatten M, Mattheus M, Johansen OE, Woerle HJ, Broedl UC, Zinman B, Investigators E-RO. Empagliflozin and Progression of Kidney Disease in Type 2 Diabetes. N Engl J Med. 2016;375(4):323-34.

14. Packer M, Anker SD, Butler J, Filippatos G, Pocock SJ, Carson P, Januzzi J, Verma S, Tsutsui H, Brueckmann M, Jamal W, Kimura K, Schnee J, Zeller C, Cotton D, Bocchi E, Bohm M, Choi DJ, Chopra V, Chuquiure E, Giannetti N, Janssens S, Zhang J, Gonzalez Juanatey JR, Kaul S, Brunner-La Rocca HP, Merkely B, Nicholls SJ, Perrone S, Pina I, Ponikowski P, Sattar N, Senni M, Seronde MF, Spinar J, Squire I, Taddei S, Wanner C, Zannad F, Investigators EM-RT. Cardiovascular and Renal Outcomes with Empagliflozin in Heart Failure. N Engl J Med. 2020;383(15):1413-24.

15. Anker SD, Butler J, Filippatos G, Ferreira JP, Bocchi E, Bohm M, Brunner-La Rocca HP, Choi DJ, Chopra V, Chuquiure-Valenzuela E, Giannetti N, Gomez-Mesa JE, Janssens S, Januzzi JL, Gonzalez-Juanatey JR, Merkely B, Nicholls SJ, Perrone SV, Pina IL, Ponikowski P, Senni M, Sim D, Spinar J, Squire I, Taddei S, Tsutsui H, Verma S, Vinereanu D, Zhang J, Carson P, Lam CSP, Marx N, Zeller C, Sattar N, Jamal W, Schnaidt S, Schnee JM, Brueckmann M, Pocock SJ, Zannad F, Packer M, Investigators EM-PT. Empagliflozin in Heart Failure with a Preserved Ejection Fraction. N Engl J Med. 2021;385(16):1451-61.

16. Heerspink HJL, Stefansson BV, Correa-Rotter R, Chertow GM, Greene T, Hou FF, Mann JFE, McMurray JJV, Lindberg M, Rossing P, Sjostrom CD, Toto RD, Langkilde AM, Wheeler DC, Committees D-CT, Investigators. Dapagliflozin in Patients with Chronic Kidney Disease. N Engl J Med. 2020;383(15):1436-46.

17. Group E-KC, Herrington WG, Staplin N, Wanner C, Green JB, Hauske SJ, Emberson JR, Preiss D, Judge P, Mayne KJ, Ng SYA, Sammons E, Zhu D, Hill M, Stevens W, Wallendszus K, Brenner S, Cheung AK, Liu ZH, Li J, Hooi LS, Liu W, Kadowaki T, Nangaku M, Levin A, Cherney D, Maggioni AP, Pontremoli R, Deo R, Goto S, Rossello X, Tuttle KR, Steubl D, Petrini M, Massey D, Eilbracht J, Brueckmann M, Landray MJ, Baigent C, Haynes R. Empagliflozin in Patients with Chronic Kidney Disease. N Engl J Med. 2022.

18. Castoldi G, Carletti R, Ippolito S, Colzani M, Barzaghi F, Stella A, Zerbini G, Perseghin G, Zatti G, di Gioia CRT. Sodium-glucose cotransporter 2 inhibition prevents renal fibrosis in cyclosporine nephropathy. Acta Diabetol. 2021;58(8):1059-70.

19. Zhang Y, Thai K, Kepecs DM, Gilbert RE. Sodium-Glucose Linked Cotransporter-2 Inhibition Does Not Attenuate Disease Progression in the Rat Remnant Kidney Model of Chronic Kidney Disease. PLoS One. 2016;11(1):e0144640.

20. Tsuprykov O, Ando R, Reichetzeder C, von Websky K, Antonenko V, Sharkovska Y, Chaykovska L, Rahnenfuhrer J, Hasan AA, Tammen H, Alter M, Klein T, Ueda S,

Yamagishi SI, Okuda S, Hocher B. The dipeptidyl peptidase inhibitor linagliptin and the angiotensin II receptor blocker telmisartan show renal benefit by different pathways in rats with 5/6 nephrectomy. Kidney Int. 2016;89(5):1049-61.

21. Zeng S, Delic D, Chu C, Xiong Y, Luo T, Chen X, Gaballa MMS, Xue Y, Chen X, Cao Y, Hasan AA, Stadermann K, Frankenreiter S, Yin L, Kramer BK, Klein T, Hocher B. Antifibrotic effects of low dose SGLT2 Inhibition with empagliflozin in comparison to Ang II receptor blockade with telmisartan in 5/6 nephrectomised rats on high salt diet. Biomed Pharmacother. 2022;146:112606.

22. Chen X, Delic D, Cao Y, Shen L, Shao Q, Zhang Z, Wu H, Hasan AA, Reichetzeder C, Gaballa MMS, Kramer BK, Klein T, Yin L, He B, Morgera S, Hocher B. Reno-protective Effects of Empagliflozin are linked to Activation of the Tubuloglomerular Feedback Mechanism and Blunting of the Complement System. Am J Physiol Cell Physiol. 2023.

23. Rajasekeran H, Lytvyn Y, Bozovic A, Lovshin JA, Diamandis E, Cattran D, Husain M, Perkins BA, Advani A, Reich HN, Kulasingam V, Cherney DZI. Urinary adenosine excretion in type 1 diabetes. Am J Physiol Renal Physiol. 2017;313(2):F184-F91.

24. Kanasaki K, Shi S, Kanasaki M, He J, Nagai T, Nakamura Y, Ishigaki Y, Kitada M, Srivastava SP, Koya D. Linagliptin-mediated DPP-4 inhibition ameliorates kidney fibrosis in streptozotocin-induced diabetic mice by inhibiting endothelial-to-mesenchymal transition in a therapeutic regimen. Diabetes. 2014;63(6):2120-31.

25. Delic D, Wiech F, Urquhart R, Gabrielyan O, Rieber K, Rolser M, Tsuprykov O, Hasan AA, Kramer BK, Baum P, Kohler A, Gantner F, Mark M, Hocher B, Klein T. Linagliptin and telmisartan induced effects on renal and urinary exosomal miRNA expression in rats with 5/6 nephrectomy. Sci Rep. 2020;10(1):3373.

26. Abbas NAT, El Salem A, Awad MM. Empagliflozin, SGLT2 inhibitor, attenuates renal fibrosis in rats exposed to unilateral ureteric obstruction: potential role of klotho expression. Naunyn Schmiedebergs Arch Pharmacol. 2018;391(12):1347-60.

27. Rajasekeran H, Reich HN, Hladunewich MA, Cattran D, Lovshin JA, Lytvyn Y, Bjornstad P, Lai V, Tse J, Cham L, Majumder S, Bowskill BB, Kabir MG, Advani SL, Gibson IW, Sood MM, Advani A, Cherney DZI. Dapagliflozin in focal segmental glomerulosclerosis: a combined human-rodent pilot study. Am J Physiol Renal Physiol. 2018;314(3):F412-F22.

28. Ma Q, Steiger S, Anders HJ. Sodium glucose transporter-2 inhibition has no renoprotective effects on non-diabetic chronic kidney disease. Physiol Rep. 2017;5(7).

29. Chu C, Lu YP, Yin L, Hocher B. The SGLT2 Inhibitor Empagliflozin Might Be a New Approach for the Prevention of Acute Kidney Injury. Kidney Blood Press Res. 2019;44(2):149-57.

30. Yamazaki D, Konishi Y, Morikawa T, Kobara H, Masaki T, Hitomi H, Osafune K, Nakano D, Kittikulsuth W, Nishiyama A. Failure to confirm a sodium-glucose cotransporter 2 inhibitor-induced hematopoietic effect in non-diabetic rats with renal anemia. J Diabetes Investig. 2020;11(4):834-43.

31. Tauber P, Sinha F, Berger RS, Gronwald W, Dettmer K, Kuhn M, Trum M, Maier LS, Wagner S, Schweda F. Empagliflozin Reduces Renal Hyperfiltration in Response to Uninephrectomy, but Is Not Nephroprotective in UNx/DOCA/Salt Mouse Models. Front Pharmacol. 2021;12:761855.

32. Thomson SC, Vallon V. Effects of SGLT2 inhibitor and dietary NaCl on glomerular hemodynamics assessed by micropuncture in diabetic rats. Am J Physiol Renal Physiol. 2021;320(5):F761-F71.

33. Kim S, Jo CH, Kim GH. Effects of empagliflozin on nondiabetic salt-sensitive hypertension in uninephrectomized rats. Hypertens Res. 2019;42(12):1905-15.

34. Lu YP, Wu HW, Zhu T, Li XT, Zuo J, Hasan AA, Reichetzeder C, Delic D, Yard B, Klein T, Kramer BK, Zhang ZY, Wang XH, Yin LH, Dai Y, Zheng ZH, Hocher B. Empagliflozin reduces kidney fibrosis and improves kidney function by alternative macrophage activation in rats with 5/6-nephrectomy. Biomed Pharmacother. 2022;156:113947.

35. Franzin R, Stasi A, Fiorentino M, Stallone G, Cantaluppi V, Gesualdo L, Castellano G. Inflammaging and Complement System: A Link Between Acute Kidney Injury and Chronic Graft Damage. Front Immunol. 2020;11:734.

36. Boor P, Konieczny A, Villa L, Schult AL, Bucher E, Rong S, Kunter U, van Roeyen CR, Polakowski T, Hawlisch H, Hillebrandt S, Lammert F, Eitner F, Floege J, Ostendorf T. Complement C5 mediates experimental tubulointerstitial fibrosis. J Am Soc Nephrol. 2007;18(5):1508-15.

37. Curci C, Castellano G, Stasi A, Divella C, Loverre A, Gigante M, Simone S, Cariello M, Montinaro V, Lucarelli G, Ditonno P, Battaglia M, Crovace A, Staffieri F, Oortwijn B, van Amersfoort E, Gesualdo L, Grandaliano G. Endothelial-to-mesenchymal transition and renal fibrosis in ischaemia/reperfusion injury are mediated by complement anaphylatoxins and Akt pathway. Nephrol Dial Transplant. 2014;29(4):799-808.

38. Delpech PO, Thuillier R, SaintYves T, Danion J, Le Pape S, van Amersfoort ES, Oortwijn B, Blancho G, Hauet T. Inhibition of complement improves graft outcome in a pig model of kidney autotransplantation. J Transl Med. 2016;14(1):277.

Statutory Declaration

"I, Xin Chen, by personally signing this document in lieu of an oath, hereby affirm that I prepared the submitted dissertation on the topic "Molecular Mechanisms of Nephroprotection of SGLT2 Inhibitor", "Molekulare Mechanismen der Nephroprotektion von SGLT2 Hemmern", independently and without the support of third parties, and that I used no other sources and aids than those stated.

All parts which are based on the publications or presentations of other authors, either in letter or in spirit, are specified as such in accordance with the citing guidelines. The sections on methodology (in particular regarding practical work, laboratory regulations, statistical processing) and results (in particular regarding figures, charts and tables) are exclusively my responsibility.

Furthermore, I declare that I have correctly marked all of the data, the analyses, and the conclusions generated from data obtained in collaboration with other persons, and that I have correctly marked my own contribution and the contributions of other persons (cf. declaration of contribution). I have correctly marked all texts or parts of texts that were generated in collaboration with other persons.

My contributions to any publications to this dissertation correspond to those stated in the below joint declaration made together with the supervisor. All publications created within the scope of the dissertation comply with the guidelines of the ICMJE (International Committee of Medical Journal Editors; http://www.icmje.org) on authorship. In addition, I declare that I shall comply with the regulations of Charité – Universitätsmedizin Berlin on ensuring good scientific practice.

I declare that I have not yet submitted this dissertation in identical or similar form to another Faculty.

The significance of this statutory declaration and the consequences of a false statutory declaration under criminal law (Sections 156, 161 of the German Criminal Code) are known to me."

Date Signature

Declaration of individual contribution to the publication

Chen, X., Delić, D., Cao, Y., Shen, L., Shao, Q., Zhang, Z., Wu, H., Hasan, A. A., Reichetzeder, C., Gaballa, M. M. S., Krämer, B. K., Klein, T., Yin, L., He, B., Morgera, S., & Hocher, B. (2023). Reno-protective Effects of Empagliflozin are linked to Activation of the Tubuloglomerular Feedback Mechanism and Blunting of the Complement System. American journal of physiology. Cell physiology, 10.1152/ajpcell.00528.2022. Advance online publication. https://doi.org/10.1152/ajpcell.00528.2022 (IF=5.282)

Xin Chen contributed the following to the publication:

I was involved throughout the study, including study design, establishment of animal models, medication gavage, sample collection, sample testing and analysis of all data. Figure 1 shows the experimental design completed under the supervision of my supervisor. After completing the animal experiments, I measured the renal function parameters (blood drug concentration, serum creatinine, urine creatinine, urine albumin) in the blood and urine of the rats and combined them with other physiological parameters to create Table 1 and Figure 2. I then performed four histological stains and analyses in the kidney tissue, including PAS, Sirius Red Staining, PASM and Masson, and produced Figure 3 to show the results of the assessment. I also examined urinary adenosine excretion rates for validation of SGLT2 inhibitors via TGF-mediated renoprotection and explored the correlation of TGF with renal function and histological parameters inspired by my supervisor. I produced Figure 4 to present the results of the analysis on TGF. Furthermore, I participated in the immunofluorescence experiments and analysis of macrophages and T cells in the study and presented the results in figure 5. In addition, I analysed the RNA sequencing data and screened the differentially expressed genes for qRT-PCR validation using Venn diagrams and volcano diagrams (Figure 6). I participated in the qRT-PCR analysis and presented the results in figure 7. After completing all the above experiments and analyses, I wrote the original manuscript and made all the additional analyses and changes based on the reviewers' comments to finalise the manuscript and publish it.

____

Signature, date and stamp of first supervising university professor / lecturer

____

Signature of doctoral candidate

Printing copy of the publication

AMERICAN JOURNAL OF PHYSIOLOGY
CELL PHYSIOLOGY

Am J Physiol Cell Physiol 324: C951–C962, 2023.
First published February 13, 2023; doi:10.1152/ajpcell.00528.2022

RESEARCH ARTICLE

Cellular and Molecular Effects of Antidiabetics Beyond Glycemic Control

Renoprotective effects of empagliflozin are linked to activation of the tubuloglomerular feedback mechanism and blunting of the complement system

Xin Chen,[1,2,3] Denis Delić,[2,4] Yaochen Cao,[1,2] Linghong Shen,[5] Qin Shao,[5] Zheyu Zhang,[3] Hongwei Wu,[3] Ahmed A. Hasan,[2,6] Christoph Reichetzeder,[7] Mohamed M. S. Gaballa,[2,8] Bernhard K. Krämer,[2,9] Thomas Klein,[10] Lianghong Yin,[3] Ben He,[5] Stanislao Morgera,[1] and Berthold Hocher[2,11,12]

[1]Department of Nephrology, Charité—Universitätsmedizin Berlin, Campus Mitte, Berlin, Germany; [2]Fifth Department of Medicine (Nephrology/Endocrinology/Rheumatology/Pneumology), University Medical Centre Mannheim, University of Heidelberg, Heidelberg, Germany; [3]The First Clinical Medical College of Jinan University, The First Affiliated Hospital of Jinan University, Guangzhou, People's Republic of China; [4]Department of Translational Medicine & Clinical Pharmacology, Boehringer Ingelheim Pharma GmbH & Co. KG, Biberach, Germany; [5]Department of Cardiology, Shanghai Chest Hospital, Shanghai Jiao Tong University School of Medicine, Shanghai, People's Republic of China; [6]Institute of Pharmacy, Freie Universität Berlin, Berlin, Germany; [7]Department of Pathology, HMU — Health and Medical University, Potsdam, Germany; [8]Faculty of Veterinary Medicine, Benha University, Toukh, Egypt; [9]European Center for Angioscience, Medical Faculty Mannheim, University of Heidelberg, Heidelberg, Germany; [10]Department of Cardiometabolic Diseases Research, Boehringer Ingelheim Pharma GmbH & Co. KG, Biberach, Germany; [11]Reproductive and Genetic Hospital of CITIC-Xiangya, Changsha, People's Republic of China; and [12]IMD Institut für Medizinische Diagnostik Berlin-Potsdam GbR, Berlin, Germany

Abstract

The mechanisms of nephroprotection in nondiabetic chronic kidney disease (CKD) models by sodium-glucose cotransporter 2 (SGLT2) inhibitors are not well defined. Five groups were established: sham-operated rats, placebo-treated rats with 5/6 nephrectomy (5/6Nx), 5/6Nx + telmisartan (5 mg/kg/day), 5/6Nx + empagliflozin (3 mg/kg/day), and 5/6Nx + empagliflozin (15 mg/kg/day). Treatment duration was 95 days. Empagliflozin showed a dose-dependent beneficial effect on the change from baseline of creatinine clearance (Ccr). The urinary albumin-to-creatinine ratio likewise improved in a dose-dependent manner. Both dosages of empagliflozin improved morphological kidney damage parameters such as renal interstitial fibrosis and glomerulosclerosis. 5/6 nephrectomy led to a substantial reduction of urinary adenosine excretion, a surrogate parameter of the tubuloglomerular feedback (TGF) mechanism. Empagliflozin caused a dose-dependent increase in urinary adenosine excretion. The urinary adenosine excretion was negatively correlated with renal interstitial fibrosis and positively correlated with Ccr. Immunofluorescence analysis revealed that empagliflozin had no effect on $CD8^+$ and $CD4^+$ T cells as well as on $CD68^+$ cells (macrophages). To further explore potential mechanisms, a nonhypothesis-driven approach was used. RNA sequencing followed by quantitative real-time polymerase chain reaction revealed that complement component 1Q subcomponent A chain (*C1QA*) as well as complement component 1Q subcomponent C chain (*C1QC*) gene expression were upregulated in the placebo-treated 5/6Nx rats and this upregulation was blunted by treatment with empagliflozin. In conclusion, empagliflozin-mediated nephroprotection in nondiabetic CKD is due to a dose-dependent activation of the TGF as well as empagliflozin-mediated effects on the complement system.

complement system; nondiabetic chronic kidney disease; sodium-glucose cotransporter 2 inhibitor; tubuloglomerular feedback

INTRODUCTION

Chronic kidney disease (CKD) arises from a number of heterogeneous disease pathways that irreversibly alter the function and structure of the kidney (1). According to worldwide estimates, there are nearly 700 million prevalent patients with chronic kidney disease(2). In addition to primary kidney disease, common chronic diseases such as hypertension and diabetes harm the kidneys and hence contribute to the burden of CKD (3). Although the causes of CKD are diverse, they all culminate in progressive glomerulosclerosis, tubular atrophy, and interstitial fibrosis (4). No pharmacological treatment approach has been found to be effective in halting or reversing the progressive progression of CKD in humans, and renal replacement therapy (dialysis or kidney transplantation) remains the main burden from a health economic

Correspondence: B. Hocher (berthold.hocher@medma.uni-heidelberg.de); B. He (heben241@126.com).
Submitted 21 November 2022 / Revised 3 February 2023 / Accepted 3 February 2023

point of view very costly treatment for the end-stage kidney disease.

Sodium-glucose cotransporter 2 (SGLT2) inhibitors are antidiabetic drugs that act primarily on SGLT2 expressed in the proximal tubule of the kidney, thereby reducing renal reabsorption of glucose and also sodium (5). These compounds have received special attention because several large-scale clinical trials have shown nephroprotective effects and a reduction in the incidence of cardiovascular events (6–9). However, most of these clinical trials were conducted in patients with diabetic nephropathy, and it is unclear to what extent the nephroprotective effect of SGLT2 inhibitors in patients results from a reduction in blood glucose. In fact, in a large clinical study with 4,304 nondiabetic patients with CKD, SGLT2 inhibitors had a beneficial effect on glomerular filtration rate (GFR) and reduced mortality (10). Another clinical study with 6,609 patients with CKD showed that empagliflozin therapy led to a lower risk of progression of kidney disease (11). This fits very well with earlier post hoc analyses of clinical trials showing that the nephroprotective effect of SGLT2 inhibitors were independent of hemoglobin A1c (HbA1c) and blood glucose levels (9). These evidences suggest that SGLT2 inhibitors are likely to have other beneficial effects independent of lowering blood glucose, but the underlying mechanisms of nephroprotective effects remain unclear. Current hypotheses mainly involve effects on inflammation(12), hypoxia (13), sympathetic nervous system (14), tubuloglomerular feedback (TGF) (15), and metabolism (16, 17). Nevertheless, there are limitations regarding these experiments, such as the fact that most animal experiments were done just in diabetic models, that drug treatment was rather short hence statements on long-term efficacy and safety could not be made. Finally, mainly hypothesis-driven approaches to prove efficacy on predefined pathways were usually used. Yet unknown mechanisms thus could not be identified.

Accordingly, the aim of this study was to investigate the effects of empagliflozin treatment in nondiabetic CKD rats (5/6 nephrectomy rat model) for 95 days on renal function and structure, as well as on body weight, and blood pressure. Two doses of empagliflozin (3 mg/kg/day and 15 mg/kg/day) were used to investigate potential dose dependency and telmisartan as the gold standard for nephroprotective effects were used (18–21). To further explore the potential underlying mechanisms, RNA sequencing was used to search for differentially expressed genes due to SGLT2 treatment. The resulting findings were then validated using quantitative real-time polymerase chain reaction (qRT-PCR).

METHODOLOGY

Experimental Animals and Protocol

Animal experiments were approved by the Animal Care and Use Committee of Jinan University, Guangzhou, PR China (IACUC-20190830-02). All animals were cared for in accordance with the Guide for the Care and Use of Laboratory Animals published by the US National Institute of Health (NIH Publication No. 85-23, revised 1996).

Male Wistar rats (15 animals per group, except for 10 animals in sham group), aged 7 wk, were purchased from Vital River Laboratory Animal Technology Co., Ltd (Beijing). The rats were kept at temperature-controlled conditions (22°C–25°C), humidity of 55 ± 5%, under 12 h light/dark cycles and were allowed access to standard rat chow and water ad libitum. The general condition of each animal was monitored daily. After 7 days of acclimatization, rats were randomly assigned into five different groups, sham operation + placebo; 5/6Nx + placebo; 5/6Nx + telmisartan (5 mg/kg/day); 5/6Nx + empagliflozin (3 mg/kg/day); 5/6Nx + empagliflozin (15 mg/kg/day) and were treated with medication for 95 consecutive days by gavage immediately after surgery until the end of the study (24 h before euthanasia). Doses of telmisartan (22, 23) and empagliflozin (24–26) were selected based on prior studies. The five-sixths nephrectomy (5/6Nx) operation under anesthesia with 2,2,2-tribromethanol (500 mg/kg ip) was performed as follows: uninephrectomy of the right kidney (Uni-Nx) at *week 1* followed by amputation of the poles of the left kidney at *week 3* (Supplemental Figs. S1 and S2). Sham operations were conducted at the same time points. The rats were weighed every fortnight. Blood pressure (BP) measurements using the tail-cuff method (BP-2000 Blood Pressure Analysis System, model BP-2000-RP-4, Visitech Systems), metabolic cages, and blood sampling were performed at *weeks 0, 7,* and *18* (Supplemental Figs. S1and S2). Urine was collected by placing the rats in metabolic cages (MC) for 24 h, and the 24 h urine volume was recorded. After centrifugation at 12,000 rpm for 10 min at 4°C, the urine supernatant was stored at −80°C for further analysis. Except for blood samples at *week 18*, that were taken from the abdominal aorta under anesthesia with 2,2,2-tribromethanol (500 mg/kg ip) and placed in blood collection tubes (BD Vacutainer SST II Advance Serum Tube with Separating Gel and Clotting Activator) during euthanasia process, blood samples at *weeks 0* and *7* were taken from retro-orbital venous plexus under anesthesia with isoflurane via chamber induction (3%), and the supernatants of blood samples were stored at −80°C after centrifugation at 3,000 rpm for 10 min at 4°C. The rats were euthanized at *week 18*. Upon euthanasia, blood samples were taken and kidneys were harvested. The kidneys were weighed and cut longitudinally into two halves: one half was fixed in 4% paraformaldehyde for further histological analysis and the other half was stored at −80°C with RNA tissue protection reagent (No.76106, Qiagen, Germany) for later analyzes.

Serum and Urine Analyses

Levels of serum creatinine and urinary creatinine were analyzed with automatic biochemical analyzer (Siemens biochemical analyzer and its Leadman reagent, Siemens, Germany). Urinary albumin levels were determined quantitatively using enzyme-linked immunosorbent assay kit (ab235642, Abcam, Cambridge, UK). Determination of urinary adenosine excretion (urine adenosine/urine creatinine) was performed as described previously (27). Plasma levels of empagliflozin were determined by high-performance liquid chromatography (HPLC), as described previously (28, 29). The urinary albumin-to-creatinine ratio (ACR) and creatinine clearance (Ccr) were calculated by formulas as follows: ACR = urinary albumin/urine creatinine; Ccr = [urinary creatinine (μmol/L) × urinary flow (mL/min)]/serum creatinine (μmol/L).

Histology

Renal tissues were embedded in paraffin after fixation in 4% paraformaldehyde for 48 h. The embedded renal tissues were cut into 2-μm-thick sections, then stained with periodic acid-Schiff staining (PAS), Sirius Red staining, periodic Schiff-methenamine staining (PASM), and Masson's trichrome staining (Masson) to evaluate glomerulosclerosis index, glomerular size, number of glomerular cells, renal interstitial fibrosis, and perivascular fibrosis index. All slides were scanned in full at ×400 magnification, and the images were viewed and analyzed by iViewer 6.3.6 (Unic Technologies, Inc., PR China). Glomerulosclerosis index was evaluated on PAS-stained slides by rating the percentage of the periodic acid-Schiff-positive areas within the glomerulus using a subjective, semiquantitative scoring system (*grades I–IV*) performed by two investigators who were blinded to the study groups. Analysis of perivascular fibrosis index was done by two blinded independent investigators using a semi-quantitative grading score (*grades I–IV*) on Masson's trichrome-stained slides as follow: *I* = weak, *II* = moderate, *III* = severe, and *IV* = very severe fibrosis per section. Images for the measurement of renal interstitial fibrosis were intercepted from full-scan images of Sirius Red staining at ×400 magnification, and the images assessed covered more than 80% of the entire slide. Subsequently, the percentage of fibrosis on these images was measured by the ImageJ threshold method (National Institutes of Health), as previously described (30). Glomerular size and number of glomerular cells were assessed by analyzing 50 glomeruli of each PASM-stained slide using iViewer 6.3.6 (Unic Technologies, Inc., PR China). For all of the aforementioned analyses, at least 80% field per slide was assessed by two blinded independent investigators, and the mean of the two scoring results was used.

Immunofluorescence Staining

For immunofluorescence, 4-μm-thick slides were used. Frozen sections were prepared and immunofluorescence analysis was conducted using primary antibodies as follows: anti-CD68 (GB113109, Servicebio, PR China, dilution 1:2,000), anti-CD8 (GB11068, Servicebio, PR China, dilution 1:500), and anti-CD4 (GB11064-1, Servicebio, PR China, dilution 1:500) overnight at 4°C. Then, the tissues and cells were washed and incubated with secondary antibody (anti-CD68: GB22303, Servicebio, PR China, dilution 1:500; anti-CD8 and anti-CD4: GB21303, Servicebio, PR China, dilution 1:300). After staining the nuclei with 4′,6-diamidino-2-phenylindole (DAPI), the tissues and cells were visualized. For each section, 12 randomized high-power fields were examined using a fluorescence microscope at ×200 magnification. Cytotoxic T cells ($CD8^+$ cells/total cells) and helper T cells ($CD4^+$ cells/total cells) were analyzed by AIpathwell (Servicebio, PR China). The relative fluorescence unit (RFU) of CD68 was assessed by ImageJ software (National Institutes of Health). When evaluating RFUs, nonconforming images are excluded: *1*) areas with an unspecific staining pattern due to the edge effect; *2*) damaged or obscured tissue areas; *3*) areas outside our focus areas; *4*) an area with indistinct nuclei staining; and *5*) areas include irrelevant tissue features like large blood vessels or large spaces.

RNA Sequencing and Quantitative Real-Time Polymerase Chain Reaction (qRT-PCR)

Six renal tissue samples from animals with a serum creatinine level close to the median serum creatinine level at study end in each group were selected for RNA sequencing analysis using a HiSeq 4000 platform device (Illumina, Inc; San Diego, CA). Library preparation, sequencing, and data analysis of messenger RNA (mRNA) were performed, as described previously (23). The 5/6Nx + placebo (PBO) group was used as a control for group comparison. Genes with an absolute value of log2(fold-change) > 1 and a *P* value <0.05 were considered as differentially expressed genes (DEGs) (Supplemental Figs. S1–S3). Results were corrected for multiple testing. The selected differentially expressed genes were ranked from lowest to highest *P* value, and the top six functional genes that were simultaneously regulated in the control (5/6Nx + PBO and 5/6Nx + TELM) and the intervention (5/6Nx + 3 mg EMPA and 5/6Nx + 15 mg EMPA) groups were validated by qRT-PCR. Using these selection criteria, top differentially expressed genes (DEGs) were retested by qRT-PCR (SDS7900HT; Thermo Fisher Scientific, Inc., Waltham, MA). Eventually, *C1QA* (complement component 1, Q subcomponent, A chain), *C1QC* (complement component 1, Q subcomponent, C chain), *FMOD* (fibromodulin), *REN* (renin), *FMO2* (flavin-containing dimethylaniline monooxygenase 2), and *RPL36* (ribosomal protein L36) were verified by qRT-PCR. These six genes were also labeled in the Volcano plot (Supplemental Figs. S1–S3).

Statistical Analysis

Data were presented as the means ± SE. Statistical analysis was performed using GraphPad Prism 6 software (GraphPad, La Jolla, CA). ROUT (Q = 1%) in GraphPad Prism 6 software was used to identify outliers. Only two outliers were excluded (one from the 5/6Nx + TELM group for creatinine clearance and the other from the +PBO group for glomerular size). For analysis of serum creatinine over the course of the study, two-way analysis of variance (two-way ANOVA) followed by the Bonferroni post hoc test was performed. In all other cases, one-way ANOVA analysis followed by the Bonferroni post hoc test was applied for comparison of normally distributed data, and the Kruskal-Wallis test followed by Dunn's post hoc test was used for nonnormally distributed data. In all cases, differences were regarded as statistically significant if $P < 0.05$.

Materials

Empagliflozin (EMPA) and telmisartan (TELM) were manufactured and supplied by Boehringer Ingelheim Pharma GmbH & Co. KG (Biberach an der Riss, Germany). Both compounds were dissolved in 0.5% wt/vol hydroxypropyl methylcellulose in water and were administered orally by gavage. Control rats received 0.5% wt/vol hydroxypropyl methylcellulose in water.

RESULTS

Physiologic and Biochemical Data

The physiological and biochemical data of the animals are shown in Table 1. There was no statistical difference in blood pressure between all groups neither at study entry nor at

Table 1. *Changes of animal characteristics from baseline*

Parameters	Sham + PBO (n = 7)	5/6Nx + PBO (n = 9)	5/6Nx + 3 mg EMPA (n = 9)	5/6Nx + 15 mg EMPA (n = 11)	5/6Nx + TELM (n = 7)
Body weight (change from baseline, g)	208.57 ± 20.75*	149.11 ± 11.60	149.56 ± 17.53	146.36 ± 7.23	139.71 ± 15.05
Rel. kidney weight (10^{-2})	0.41 ± 0.02	0.51 ± 0.06	0.55 ± 0.05	0.61 ± 0.03	0.41 ± 0.03
Serum creatinine (change from baseline, µmol/L)	5.71 ± 0.81****	53.78 ± 8.85	23.00 ± 4.94***	22.91 ± 2.29***	37.14 ± 3.46
Final ACR (mg/g × 10^{-2})	6.66 ± 3.83*	61.75 ± 28.79	24.28 ± 7.85	8.48 ± 1.70*	6.88 ± 3.10*
Ccr (change from baseline, mL/min)	0.86 ± 0.28***	−0.99 ± 0.27	−0.11 ± 0.21	0.56 ± 0.18**	−0.50 ± 0.29
T_{24} (empagliflozin, nM)	–	–	–	23.20 ± 6.50	–

Body weight (change from baseline) = final body weight − baseline body weight; rel. kidney weight (relative kidney weight) = kidney weight/final body weight; ACR (urinary albumin-to-creatinine ratio) = urinary albumin/urine creatinine; Ccr (creatinine clearance) = [urinary creatinine (µmol/L) × urinary flow (mL/min)]/serum creatinine (µmol/L); Ccr (change from baseline) = final Ccr − baseline Ccr; T_{24} (empagliflozin, nM): plasma concentrations of empagliflozin after 24 h of gavage. – indicates below the minimum detection value. Values displayed are means ± SE. $^*P < 0.05$; $^{**}P < 0.01$; $^{***}P < 0.001$; $^{****}P < 0.0001$, significantly different from 5/6Nx + PBO. EMPA, empagliflozin; 5/6Nx, 5/6 nephrectomized rat model; PBO, placebo; Sham, sham operation; TELM, telmisartan.

study end (data not shown). Empagliflozin demonstrated a dose-dependent beneficial effect on the change from baseline of Ccr. The lower dose of empagliflozin showed only a trend toward improvement compared with placebo. The overall picture, however, indicates a dose dependency of the empagliflozin effects on Ccr. The urinary albumin-to-creatinine ratio was determined only at the end of the experiment. Here, too, a dose-dependent beneficial effect of empagliflozin can be seen. The nephroprotective effects of empagliflozin at the higher dose were superior to treatment effects of a standard dose of the angiotensin II receptor blocker telmisartan, the current gold standard for the treatment of CKD (Table 1 and Fig. 1).

Kidney Morphology

All histological parameters of kidney damage (renal interstitial fibrosis, perivascular fibrosis index, glomerulosclerosis index, number of glomerular cells and glomerular size) were clearly pronounced after 5/6Nx compared with the sham-operated rats (Fig. 2, *A–F*). Both the low and high doses of empagliflozin improved all these morphological kidney damage parameters (Fig. 2, *A–F*). Treatment with both dosages of empagliflozin led to an almost complete regression of the pathological changes of renal interstitial fibrosis, perivascular fibrosis index, glomerulosclerosis index, and number of glomerular cells (Fig. 2, *A–E* and Supplemental Fig. S2). The effect on glomerular size was significant, but less pronounced. Here, as with the functional parameters, see Fig. 1, some dose dependency was suggested (Fig. 2*F*). The angiotensin II receptor blocker telmisartan improved all analyzed kidney damage parameters significantly (Fig. 2, *A–F*).

Urinary Adenosine

The 5/6 nephrectomy led to a drastic reduction in urinary adenosine excretion. Empagliflozin induced a dose-dependent increase in urinary adenosine excretion. The higher dose group of empagliflozin was significantly different from placebo-treated rats with 5/6 nephrectomy in terms of urinary adenosine excretion (Fig. 3*A*). Telmisartan treatment showed a trend toward increasing the urine adenosine to urine creatinine ratio (P = 0.057, Fig. 3*A*). Urinary adenosine to creatinine ratio at study end was negatively correlated with renal interstitial fibrosis (Fig. 3*B*) and glomerular size (Fig. 3*C*) and positively correlated with Ccr at study end (Fig. 3*D*).

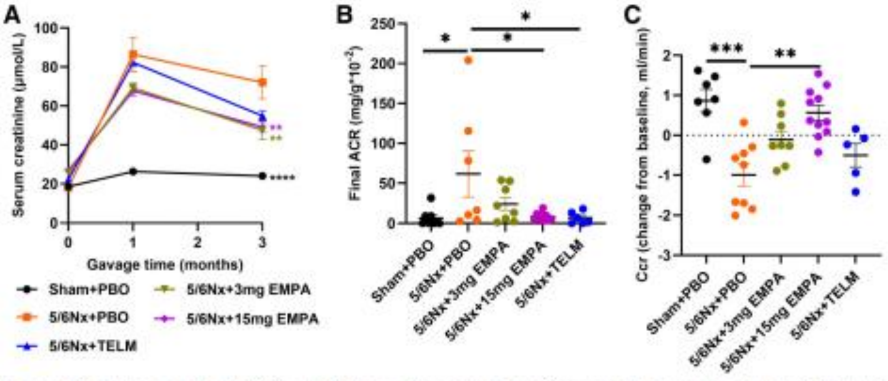

Figure 1. Effect on renal function compared with 5/6Nx + PBO group. *A*: concentrations of serum creatinine over the course of the study: Sham + PBO (n = 7), 5/6Nx + 3 mg EMPA (n = 8) and 5/6Nx + 15 mg EMPA (n = 11) were lower than 5/6Nx + PBO (n = 9). *B*: final ACR: Sham + PBO (n = 8), 5/6Nx + 15 mg EMPA (n = 9) and 5/6Nx + TELM (n = 6) were lower than 5/6Nx + PBO (n = 7). *C*: Ccr (change from baseline): Sham + PBO (n = 7) and 5/6Nx + 15 mg EMPA (n = 11) were higher than 5/6Nx + PBO (n = 9). Values displayed are means ± SE. $^*P < 0.05$; $^{**}P < 0.01$; $^{***}P < 0.001$; $^{****}P < 0.0001$, significantly different from 5/6Nx + PBO. EMPA, empagliflozin; 5/6Nx, 5/6 nephrectomized rat model; PBO, placebo; Sham, sham operation; TELM, telmisartan. ACR, urinary albumin-to-creatinine ratio; Ccr, creatinine clearance.

AJP-Cell Physiol • doi:10.1152/ajpcell.00528.2022 • www.ajpcell.org

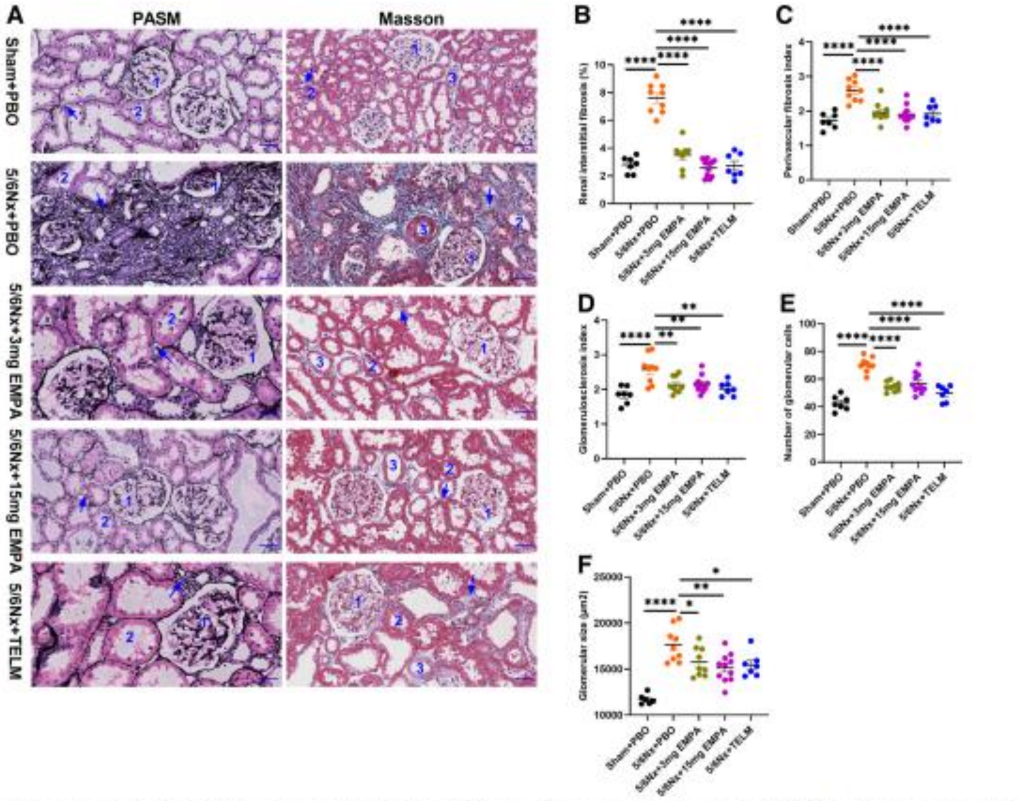

Figure 2. Histopathological analysis of kidney compared with 5/6Nx + PBO group. *A*: representative micrographs of PASM and Masson staining of kidney sections from each group (×400, scale bar = 50 μm); *Label 1*: glomerulus; *Label 2*: renal tubules; *Label 3*: vascular; arrow: renal interstitial fibrosis. Renal interstitial fibrosis (%; *B*); perivascular fibrosis index (*C*); glomerulosclerosis index (*D*); number of glomerular cells (*E*); glomerular size (μm^2; *F*). All these indicators were lower in the other groups [Sham + PBO ($n = 7$), 5/6Nx + TELM ($n = 7$), 5/6Nx + 3 mg EMPA ($n = 9$) and 5/6Nx + 15 mg EMPA ($n = 11$)] than in the 5/6Nx + PBO ($n = 9$) group. Values displayed are means ± SE. $*P < 0.05$; $**P < 0.01$; $***P < 0.001$; $****P < 0.0001$, significantly different from 5/6Nx + PBO. EMPA, empagliflozin; 5/6Nx, 5/6 nephrectomized rat model; PASM, periodic Schiff-methenamine staining; PBO, placebo; Sham, sham operation; TELM, telmisartan.

Kidney Immunofluorescence

Some studies (31, 32), including our own recently published study (33), suggest that SGLT2 inhibitor ameliorates renal fibrosis in CKD rats by affecting macrophage and inflammatory cells. We therefore detect the number of $CD4^+$ and $CD8^+$ cells, as well as the CD68+ cells in kidney tissues. However, there were no statistical differences between 5/6Nx + PBO and the other groups with regard to kidney tissue density of cytotoxic T cells ($CD8^+$ cells/total cells) and T helper cells ($CD4^+$ cells/total cells) (Fig. 4, *A–C*). The tissue density of CD68+ cells (macrophages) was increased in 5/6Nx + PBO group ($P = 0.047$) versus sham-operated animal. However, neither empagliflozin nor telmisartan treatment had an effect on the tissue density of macrophages after 5/6 nephrectomy (Fig. 4*D*). Taken together, neither empagliflozin nor telmisartan had an effect on $CD8^+$ T cells and $CD4^+$ T cells, and also on CD68+ cells (macrophages).

RNA Sequencing and Quantitative Real-Time Polymerase Chain Reaction (qRT-PCR) of Kidney Samples

Venn diagram between 5/6Nx + 3 mg EMPA, 5/6Nx + 15 mg EMPA and 5/6Nx + PBO groups showed 4 coregulated genes between these three groups, 73 coregulated genes between 5/6Nx + 3 mg EMPA and 5/6Nx + PBO groups, and 11 coregulated genes between 5/6Nx + 15 mg EMPA and 5/6Nx + PBO groups (Fig. 5*A*). Using the selection criteria (top-fold-change, detection in several comparisons, and known function, for details, see method section), RNA sequencing yielded six candidate genes for verification with qRT-PCR in all samples: complement component 1Q subcomponent A chain (*CIQA*); complement component 1Q subcomponent C chain (*CIQC*); fibromodulin (*FMOD*); renin (*REN*); flavin-containing dimethylaniline monooxygenase 2 (*FMO2*); and ribosomal protein L36 (*RPL36*) (Supplemental Figs. S1–S3 and Fig.

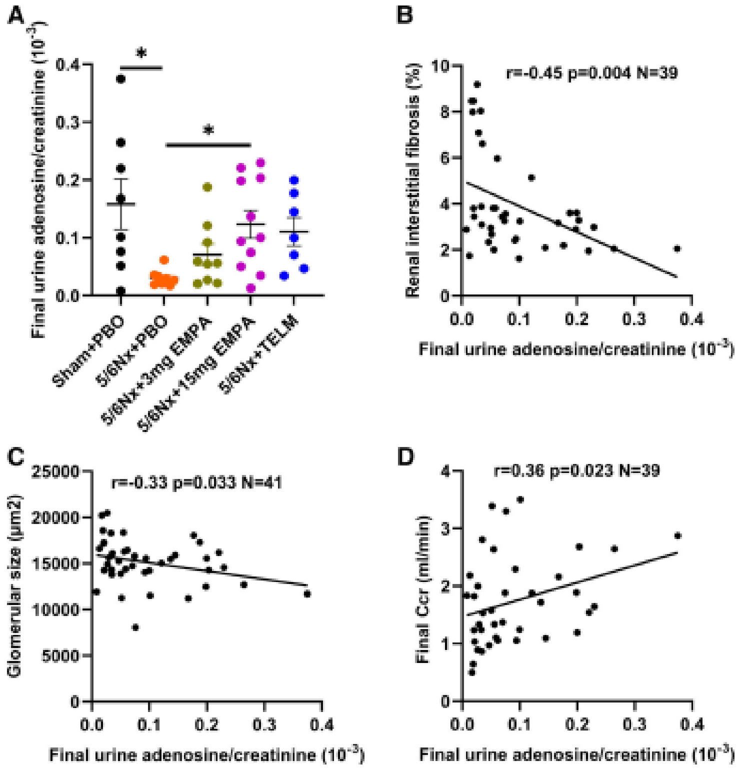

Figure 3. *A*: comparison of final urine adenosine/urine creatinine between each treatment group and 5/6Nx + PBO. Values displayed are means ± SE. $*P < 0.05$, significantly different from 5/6Nx + PBO. Inverse correlation between urinary adenosine/creatinine ratio at study end with renal interstitial fibrosis ($r = -0.45$, $P = 0.004$, $N = 39$; *B*) and glomerular size ($r = -0.33$ $P = 0.033$ $N = 41$; *C*). Positive correlation between urinary adenosine/creatinine ratio at study end with GFR ($r = 0.36$, $P = 0.023$, $N = 39$; *D*). EMPA, empagliflozin; 5/6Nx, 5/6 nephrectomized rat model; PBO, placebo; Sham, sham operation; TELM, telmisartan. Ccr, creatinine clearance.

5). Only the *CIQA* and *CIQC* genes showed a model effect—means were upregulated after 5/6 nephrectomy—and responded to empagliflozin treatment (Fig. 5, *B* and *C*). Renin expression was not altered significantly by 5/6 nephrectomy but increased substantially after treatment with the angiotensin II receptor blocker telmisartan, a well-known effect of telmisartan (34, 35).

DISCUSSION

This study provides evidence of a dose-dependent, glucose-independent nephroprotection by the SGLT2 inhibitor empagliflozin. These nephroprotective effects of the SGLT2 inhibition were accompanied by dose-dependent effects on a surrogate parameter of the TGF mechanism: urinary adenosine excretion. Besides that, whole genome RNA sequencing followed by qRT-PCR confirmation identified alterations in gene expression of key genes of the complement system in the kidney. Activation of the complement system has been shown to be a key mechanism of kidney injury.

Our data on the nephroprotective effects of SGLT2 inhibition by empagliflozin fits to previous findings in patients with diabetes (8–10) and also to findings in animal models of diabetic nephropathy (36–38) and even to findings in nondiabetic nephropathy models (39–43). However, there are also some studies showing no effect of SGLT2 inhibition in nondiabetic CKD models. Nishiyama et al. (44) found that SGLT2 inhibitor (TA-1887, 10 mg/kg/day) treatment of 5/6 nephrectomized rats for 10 wk had no beneficial effects on serum creatinine clearance, proteinuria and renal tissue structure. Gilbert and colleagues (45) showed that 0.5 mg/kg dapagliflozin twice/day for 12 wk had no effect on renal function or structure in 5/6 nephrectomized rats. Since different dosages were not tested in current studies, one might speculate that dosing in these studies or compound-related effects could account for these differences. The effects of different SGLT2 inhibitor compounds may also vary. Some current clinical studies showed that empagliflozin is more effective than dapagliflozin (46, 47). Besides that, the choice of the CKD model seems to matter. Tauber et al. (48) using an adenine-induced CKD model and Vervaet and colleagues (49) using a CKD model with unilateral nephrectomy on high-salt diets detected no beneficial response to SGLT2 inhibition. In clinical practice, however, SGLT2 inhibitors seem to decrease chronic kidney disease progression independently of the underlying type of initial kidney injury.

It was suggested that the nephroprotective effects of the SGLT2 inhibitor empagliflozin are most likely due to its effect on the tubuloglomerular feedback (TGF) mechanism (14, 50, 51). The TGF regulates glomerular blood flow and hence glomerular. This is a physiological counter-regulation that protects individual nephrons from hyperfiltration,

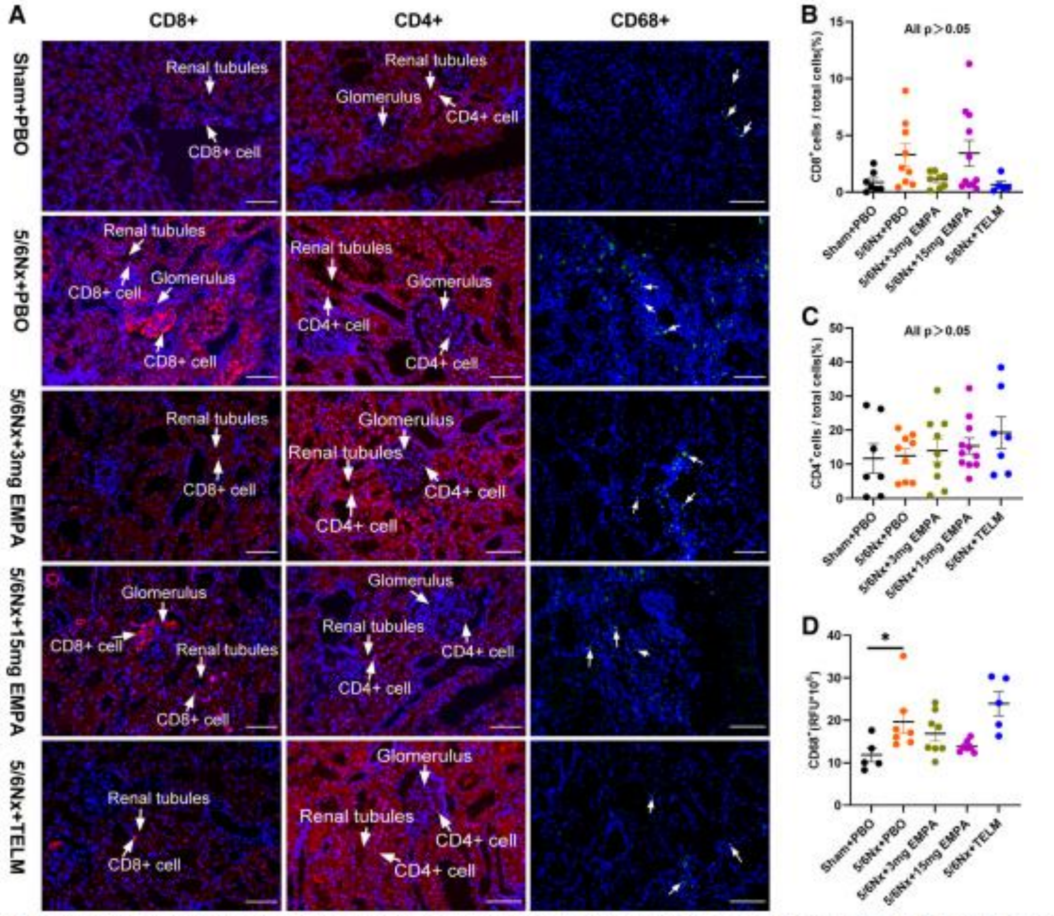

Figure 4. Immunofluorescence staining analysis of kidney. *A*: representative micrographs of kidney sections from each treatment group (×200, scale bar = 100 μm). *B*: cytotoxic T cells ($CD8^+$ cells/total cells, %): no statistical difference between groups (Sham + PBO: n = 7, 5/6Nx + TELM: n = 7, 5/6Nx + 3 mg EMPA: n = 9; 5/6Nx + 15 mg EMPA: n = 11; 5/6Nx + PBO: n = 9). *C*: helper T cells ($CD4^+$ cells/total cells, %): no statistical difference between groups (Sham + PBO: n = 7, 5/6Nx + TELM: n = 7, 5/6Nx + 3 mg EMPA: n = 9; 5/6Nx + 15 mg EMPA: n = 11; 5/6Nx + PBO: n = 9). *D*: macrophages (CD68+, RFU): 5/6Nx + PBO was higher than Sham + PBO group (Sham + PBO: n = 5, 5/6Nx + TELM: n = 5, 5/6Nx + 3 mg EMPA: n = 8; 5/6Nx + 15 mg EMPA: n = 7; 5/6Nx + PBO: n = 7). The arrows point to CD68+ cells. Values displayed are means ± SE. *$P < 0.05$, significantly different from 5/6Nx + PBO. EMPA, empagliflozin; 5/6Nx, 5/6 nephrectomized rat model; PBO, placebo; RFU, relative fluorescence unit; Sham, sham operation; TELM, telmisartan.

increased intraglomerular pressure and sodium and fluid overload of the tubules. TGF is based on the osmosensory cells of the macula densa, which are part of the juxtaglomerular apparatus. They measure the concentration of sodium and chloride ions in the lumen of the distal tubule via the Na-K-2Cl cotransporter (52–54). Huge amounts of the filtered sodium in the glomerulus are reabsorbed in the S1 segment of the proximal tubule of the nephron by a transporter called sodium-glucose cotransporter 2 (SGLT2). Inhibition of SGLT2 in the S1 segment of the proximal tubule leads to increased sodium at the macula densa of the distal tubule, which causes constriction of the afferent arteriole and reduction of glomerular filtration pressure via paracrine signaling pathways (55, 56). Recent study data from patients with type 2 diabetes mellitus (T2DM) also suggest a dilating effect at the efferent arteriole with the same end effect of intraglomerular pressure reduction and decreasing hyperfiltration (57, 58). Reduction of intraglomerular pressure is a key factor for decreasing chronic loss of kidney function. In other words, in response to SGLT2 inhibition, less sodium and glucose are taken up in the proximal tubules by the SGLT2 and pass through the Henle loop, thus more sodium and glucose are seen by the macula densa with subsequently more adenosine generation, which increases afferent

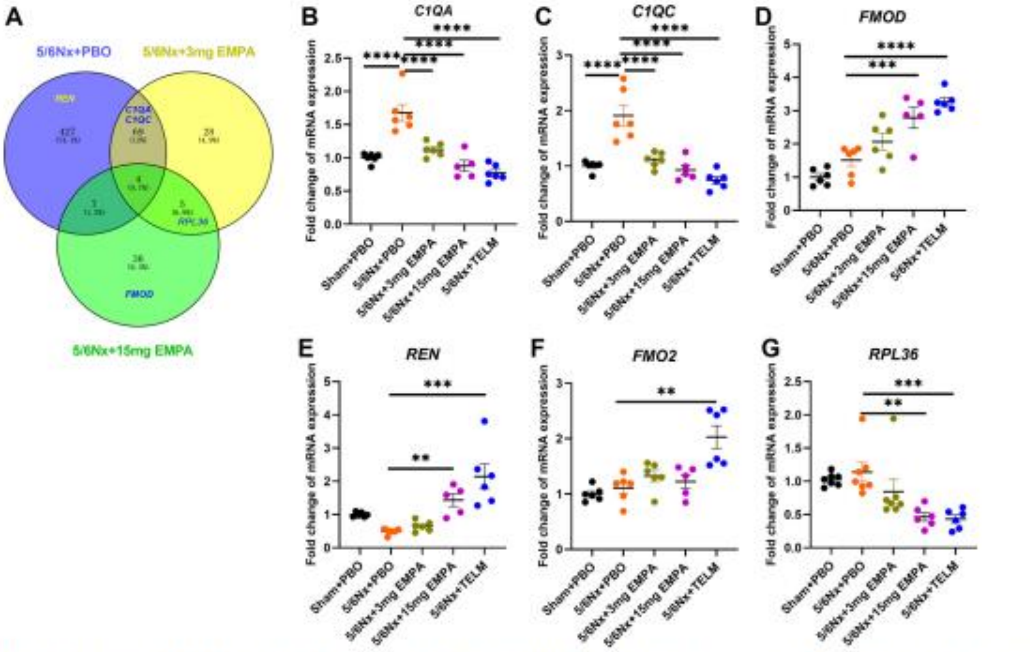

Figure 5. Gene expression in the kidney identified by qRT-PCR. *A*: Venn diagram of the differentially expressed genes from RNA-seq transcriptome for 5/6Nx + PBO, 5/6Nx + 3 mg EMPA and 5/6Nx + 15 mg EMPA groups. The circles represent the total number of statistically significant different genes [P value < 0.05 and an absolute value of log2(fold-change) > 1] in 5/6 Nx + 3 mg EMPA and 5/6 Nx + 15 mg EMPA groups in comparison to 5/6 Nx + PBO in kidney according to RNA-seq transcriptome data. *B*: fold-change of *C1QA* expression (complement component 1, Q subcomponent, A chain). *C*: fold-change of *C1QC* expression (complement component 1, Q subcomponent, C chain). *D*: fold-change of *FMOD* expression (fibromodulin). *E*: fold-change of *REN* expression (renin). *F*: fold-change of *FMO2* expression (flavin-containing dimethylaniline monooxygenase 2). *G*: fold-change of *RPL36* expression (ribosomal protein L36). Values displayed are means ± SE. $^{**}P < 0.01$; $^{***}P < 0.001$; $^{****}P < 0.0001$, significantly different from 5/6Nx + PBO. EMPA, empagliflozin; 5/6Nx, 5/6 nephrectomized rat model; PBO, placebo; qRT-PCR, quantitative reverse transcription polymerase chain reaction; Sham, sham operation; TELM, telmisartan.

arteriole tone and decreases potentially efferent arteriole tone, hence reducing blood flow through the glomeruli and ultimately decreasing intraglomerular pressure (50, 51, 59). Decreasing intraglomerular pressure is one of the key pharmacological targets to protect the kidneys. Renin-angiotensin-aldosterone system (RAAS) blockers likewise protect the kidneys by decreasing intraglomerular pressure (60–63). Sensing the concentration of sodium and chloride ions in the lumen of the distal tubule via the Na^{+}/K^{+}-ATPase is an active process with ATP consumption. During ATP depletion, adenosine is formed. Adenosine binds to adenosine receptors (G-protein-coupled receptor) on the vascular smooth muscle cells of the afferent and efferent arteriole of the glomeruli thus reducing glomerular blood flow and intraglomerular pressure (64–66). Urinary adenosine excretion is a reliably indirect way to monitor drug effects on the TGF and was therefore used in our study (67–70). Our study was clearly able to link SGLT2 inhibitor-associated kidney protection in a classical nondiabetic CKD model to urinary adenosine excretion (Fig. 3). The correlation between Ccr, renal interstitial fibrosis, and glomerular size at study end with the urinary adenosine to creatinine ratio showed for the first time the relation between functional and structural hallmarks of CKD and urinary adenosine excretion as a surrogate parameter of the activity of the TGF. To finally prove the impact of an altered TGF by SGLT2 blockade on CKD outcome parameters, the investigation of the effects of the SGLT2 blocker in animal models without a TGF such as adenosine-1 receptor knockout mice would be helpful. Our current findings concerning TGF are in contrast to an earlier study of our group using also the 5/6 nephrectomy animal model and the same technical tools to investigate the empagliflozin effects. The only but key difference was the salt content of the food. In the previous study we gave a high-salt diet, whereas now we used the standard low-salt diet for rats. Our previous study showed no effect of empagliflozin on the urinary adenosine excretion in 5/6 nephrectomized rats on high-salt diet (29). The TGF mechanism as a target of SGLT2 blockade seems to be salt dependent—under high nutritional salt conditions, empagliflozin-mediated nephroprotective effects appeared to be TGF independent, whereas under normal salt intake, the TGF seems to play a key role (Fig. 3).

Other studies (39, 40, 43, 71–73), however, including our own recently published study (33), suggest that SGLT2 inhibition additionally ameliorates renal fibrosis in CKD rats by limiting macrophage differentiation and reducing infiltration of inflammatory cells and local expression of inflammatory factors. However, findings are controversial possibly partially due to the applied methods of investigating empagliflozin effects on inflammation. In our previous study, for example, we just applied single-cell RNA sequencing of the kidneys in a subset of animals due to budget restrictions without confirmation of findings by a second independent technology (33). We therefore now used a more sensitive method, immunofluorescence staining in all animals, to detect the number of $CD4^+$ and $CD8^+$ cells, as well as the relative fluorescence unit (RFU) of $CD68^+$ cells in kidney tissues. There was no statistical difference in $CD4^+$ and $CD8^+$ T cells as well as $CD68^+$ cells between groups (Fig. 4). Our current data are in agreement with a study analyzing the effects of 8 wk treatment with another SGLT2 blocker dapagliflozin of a nondiabetic CKD rat model (73). The reasons for overall controversial findings might be at least partially due to the methods used to detect inflammation, the CKD models used and timing of investigation after kidney injury as well as treatment duration with the SGLT2 blocker. Most of the previous studies were performed in diabetic models, whereas immunohistochemistry was more commonly used in nondiabetic models (40, 43, 72). In addition, in our current study treatment duration was 95 days, which is longer than in most other experiments. Inflammation might play no major pathophysiological role at this late stage anymore. Recently just differences in the expression of subtypes of macrophages were seen, an overall analysis of the density of macrophages might be a too crude tool to detect this (33). Given the complexity of findings reported concerning the mechanism of SGLT2 inhibition, we used additionally an open—nonhypothesis-driven approach—i.e., RNA sequencing followed by qRT-PCR to confirm findings from RNA sequencing. This strategy showed that components of the complement system—*C1QA* and *C1QC* mRNAs—were upregulated after 5/6 nephrectomy and this was corrected by empagliflozin in a dose-dependent manner (Fig. 5, *B* and *C*). *C1QA* and *C1QC* belong to *C1Q* (complement component 1Q subcomponent), the first component of complement that plays a crucial role in innate and adaptive immune responses (74). The activation of the complement system and the interaction between its components lead to a complement cascade reaction. Upregulated *C1Q* promotes the formation of its downstream C3 convertase (75) and stimulates the release of interleukin-12 (IL-12) (76), which ultimately produces the anaphylatoxins C3a and C5a via a downstream complement cascade reaction and the formation of the membrane attack complex. C3a and C5a play an important role on mediating the inflammatory and fibrotic process in the kidney (77–80). Some studies have already shown that *C1Q*-mediated increased synthesis of cytokines could further contribute to fibrosis by amplifying the interstitial inflammatory environment (81, 82). Interference with these mechanisms might likewise contribute to the beneficial effects of empagliflozin on CKD progression.

Limitations

There are still some limitations to our experiment. First of all, the 5/6 nephrectomy model is an advanced model of chronic kidney disease, and therefore the results may not be generalizable to early stages of chronic kidney disease. Second, the effects of oral drugs are systemic, so there may be other mechanisms to improve renal function beyond the kidney, such as improvements in cardiac function and effects on metabolism, but we have only investigated the structure and function of the kidney. Furthermore, some clinical trials have shown changes in GFR over time, so that TGF may reset over time in response to SGLT2 inhibition, but we only measured urinary adenosine concentrations in rats at the end of the experiment. In addition, GFR was not directly measured, but it was roughly estimated by creatinine clearance calculated from urinary and blood concentrations of creatinine. Our experiments suggest two mechanisms of renoprotection by empagliflozin—TGF-mediated effects and alterations of gene expression of key components of the complement system; however, we did not explore the relationship between TGF and the complement system in further experiments, for example by blocking the TGF or analyzing the effects of empagliflozin in animal models without an intact TGF to observe potential TGF-related changes in the complement system. Moreover, the observed alterations in the mRNA expression of *C1QA* and *C1QC* genes could also be a secondary treatment effect, means secondary to primary effects of empagliflozin on for example renal fibrosis. Finally, we primarily focused on the pure effect of the treatment with an SGLT2 blocker in this study. But the combination of an SGLT2 blocker with an angiotensin receptor blocker would be of pharmacological as well as pathophysiological interest as well.

Conclusions

Our experiments demonstrate that the nephroprotective effects of empagliflozin are not limited to diabetic nephropathy, but also improve the structure and function of nondiabetic nephropathy, including lowering serum creatinine, reducing proteinuria, increasing Ccr, and improving renal interstitial inflammation, renal interstitial fibrosis, perivascular fibrosis, and glomerulosclerosis. The nephroprotective effect of empagliflozin was more pronounced at higher doses (15 mg/kg/day) suggesting that this effect may be dose-dependent. Furthermore, the effects on urinary adenosine excretion suggest likewise a dose dependency of the effects of empagliflozin on the TGF. This suggests that the TGF-mediated effects on normalization of the glomerular pressure/glomerular hemodynamics might contribute to the nephroprotective effects of empagliflozin in a dose-dependent manner. Beyond the TGF effects, whole genome RNA sequencing followed by qRT-PCR of differently expressed genes in the kidneys suggest that empagliflozin limits complement cascade-mediated renal tissue damage in nondiabetic CKD by downregulating the expression of complement components *C1QA* and *C1QC* thus contributing to the SGLT2 blocker related amelioration of CKD progression.

DATA AVAILABILITY

The data supporting the findings of this study are available in an online database. Raw data has been stored in figshare (raw data: https://doi.org/10.6084/m9.figshare.21587529.v1;

Supplemental Figs. S1, S2, and S3: https://doi.org/10.6084/m9.figshare.21997511.v1).

SUPPLEMENTAL DATA

Supplemental Figs. S1–S3: https://doi.org/10.6084/m9.figshare.21997511.v1.

GRANTS

China Scholarship Council supported X.C. and Y.C.

DISCLOSURES

B.K.K. reports lecture fees and/or advisory board memberships and/or study participation from Astellas, Bayer, Boehringer Ingelheim, Chiesi, Riepharm, Pfizer, Sanofi, Servier and Vifor Pharma, all not related to the submitted work. D.D. and T.K. are research employees of Boehringer Ingelheim. None of the other authors has any conflicts of interest, financial or otherwise, to disclose.

AUTHOR CONTRIBUTIONS

B. Hocher conceived and designed research; X.C., Y.C., Z.Z., H.W., and L.Y. performed experiments; X.C., D.D., Y.C., L.S., Q.S., H.W., A.A.H., M.M.S.G., B.K.K., T.K., L.Y., B. He and B. Hocher analyzed data; X.C., D.D., Y.C., L.S., Q.S., A.A.H., B.K.K., T.K., and B. Hocher interpreted results of experiments; X.C., M.M.S.G., and B.K.K. prepared figures; X.C. and B. Hocher drafted manuscript; X.C., D.D., A.A.H., C.R., B.K.K., T.K., B. He, S.M., and B. Hocher edited and revised manuscript; X.C., D.D., Y.C., L.S., Q.S., Z.Z., A.A.H., B.K.K., T.K., B. He, S.M., and B. Hocher approved final version of manuscript.

REFERENCES

1. **Stevens PE, Levin A; Kidney Disease: Improving Global Outcomes Chronic Kidney Disease Guideline Development Work Group Members.** Evaluation and management of chronic kidney disease: synopsis of the kidney disease: improving global outcomes 2012 clinical practice guideline. *Ann Intern Med* 158: 825–830, 2013. doi:10.7326/0003-4819-158-11-201306040-00007.
2. **Webster AC, Nagler EV, Morton RL, Masson P.** Chronic kidney disease. *Lancet* 389: 1238–1252, 2017. doi:10.1016/S0140-6736(16)32064-5.
3. **Drawz P, Rahman M.** Chronic kidney disease. *Ann Intern Med* 162: ITC1–ITC16, 2015. doi:10.7326/AITC201506020.
4. **Rayego-Mateos S, Valdivielso JM.** New therapeutic targets in chronic kidney disease progression and renal fibrosis. *Expert Opin Ther Targets* 24: 655–670, 2020. doi:10.1080/14728222.2020.1762173.
5. **Nespoux J, Vallon V.** SGLT2 inhibition and kidney protection. *Clin Sci (Lond)* 132: 1329–1339, 2018. doi:10.1042/CS20171298.
6. **Neal B, Perkovic V, Mahaffey KW, de Zeeuw D, Fulcher G, Erondu N, Shaw W, Law G, Desai M, Matthews DR, Group CPC; CANVAS Program Collaborative Group.** Canagliflozin and cardiovascular and renal events in type 2 diabetes. *N Engl J Med* 377: 644–657, 2017. doi:10.1056/NEJMoa1611925.
7. **Wiviott SD, Raz I, Bonaca MP, Mosenzon O, Kato ET, Cahn A, Silverman MG, Zelniker TA, Kuder JF, Murphy SA, Bhatt DL, Leiter LA, McGuire DK, Wilding JPH, Ruff CT, Gause-Nilsson IAM, Fredriksson M, Johansson PA, Langkilde AM, Sabatine MS; DECLARE-TIMI 58 Investigators.** Dapagliflozin and cardiovascular outcomes in type 2 diabetes. *N Engl J Med* 380: 347–357, 2019. doi:10.1056/NEJMoa1812389.
8. **Zinman B, Wanner C, Lachin JM, Fitchett D, Bluhmki E, Hantel S, Mattheus M, Devins T, Johansen OE, Woerle HJ, Broedl UC, Inzucchi SE; EMPA-REG OUTCOME Investigators.** Empagliflozin, cardiovascular outcomes, and mortality in type 2 diabetes. *N Engl J Med* 373: 2117–2128, 2015. doi:10.1056/NEJMoa1504720.
9. **Wanner C, Inzucchi SE, Lachin JM, Fitchett D, von Eynatten M, Mattheus M, Johansen OE, Woerle HJ, Broedl UC, Zinman B; EMPA-REG OUTCOME Investigators.** Empagliflozin and progression of kidney disease in type 2 diabetes. *N Engl J Med* 375: 323–334, 2016. doi:10.1056/NEJMoa1515920.
10. **Heerspink HJL, Stefansson BV, Correa-Rotter R, Chertow GM, Greene T, Hou FF, Mann JFE, McMurray JJV, Lindberg M, Rossing P, Sjostrom CD, Toto RD, Langkilde AM, Wheeler DC; DAPA-CKD Trial Committees and Investigators.** Dapagliflozin in patients with chronic kidney disease. *N Engl J Med* 383: 1436–1446, 2020. doi:10.1056/NEJMoa2024816.
11. **Herrington WG, Staplin N, Wanner C, Green JB, Hauske SJ, Emberson JR, et al; The EMPA-KIDNEY Collaborative Group.** Empagliflozin in patients with chronic kidney disease. *N Engl J Med* 388: 117–127, 2022. doi:10.1056/NEJMoa2204233.
12. **Packer M.** Interplay of adenosine monophosphate-activated protein kinase/sirtuin-1 activation and sodium influx inhibition mediates the renal benefits of sodium-glucose co-transporter-2 inhibitors in type 2 diabetes: a novel conceptual framework. *Diabetes Obes Metab* 22: 734–742, 2020. doi:10.1111/dom.13961.
13. **Packer M.** Mechanisms leading to differential hypoxia-inducible factor signaling in the diabetic kidney: modulation by SGLT2 inhibitors and hypoxia mimetics. *Am J Kidney Dis* 77: 280–286, 2021. doi:10.1053/j.ajkd.2020.04.016.
14. **Mima A.** Sodium-glucose cotransporter 2 inhibitors in patients with non-diabetic chronic kidney disease. *Adv Ther* 38: 2201–2212, 2021. doi:10.1007/s12325-021-01735-5.
15. **Thomson SC, Vallon V.** Effects of SGLT2 inhibitor and dietary NaCl on glomerular hemodynamics assessed by micropuncture in diabetic rats. *Am J Physiol Renal Physiol* 320: F761–F771, 2021. doi:10.1152/ajprenal.00552.2020.
16. **Thomas MC, Cherney DZI.** The actions of SGLT2 inhibitors on metabolism, renal function and blood pressure. *Diabetologia* 61: 2098–2107, 2018. doi:10.1007/s00125-018-4669-0.
17. **Szekeres Z, Toth K, Szabados E.** The effects of SGLT2 inhibitors on lipid metabolism. *Metabolites* 11: 87, 2021. doi:10.3390/metabo11020087.
18. **Ruggenenti P, Perna A, Gherardi G, Garini G, Zoccali C, Salvadori M, Scolari F, Schena FP, Remuzzi G.** Renoprotective properties of ACE-inhibition in non-diabetic nephropathies with non-nephrotic proteinuria. *Lancet* 354: 359–364, 1999. doi:10.1016/S0140-6736(98)10363-X.
19. **Hou FF, Zhang X, Zhang GH, Xie D, Chen PY, Zhang WR, Jiang JP, Liang M, Wang GB, Liu ZR, Geng RW.** Efficacy and safety of benazepril for advanced chronic renal insufficiency. *N Engl J Med* 354: 131–140, 2006. doi:10.1056/NEJMoa053107.
20. **Brenner BM, Cooper ME, de Zeeuw D, Keane WF, Mitch WE, Parving HH, Remuzzi G, Snapinn SM, Zhang Z, Shahinfar S; RENAAL Study Investigators.** Effects of losartan on renal and cardiovascular outcomes in patients with type 2 diabetes and nephropathy. *N Engl J Med* 345: 861–869, 2001. doi:10.1056/NEJMoa011161.
21. **Lewis EJ, Hunsicker LG, Clarke WR, Berl T, Pohl MA, Lewis JB, Ritz E, Atkins RC, Rohde R, Raz I; Collaborative Study Group.** Renoprotective effect of the angiotensin-receptor antagonist irbesartan in patients with nephropathy due to type 2 diabetes. *N Engl J Med* 345: 851–860, 2001. doi:10.1056/NEJMoa011303.
22. **Tsuprykov O, Ando R, Reichetzeder C, von Websky K, Antonenko V, Sharkovska Y, Chaykovska L, Rahnenfuhrer J, Hasan AA, Tammen H, Alter M, Klein T, Ueda S, Yamagishi SI, Okuda S, Hocher B.** The dipeptidyl peptidase inhibitor linagliptin and the angiotensin II receptor blocker telmisartan show renal benefit by different pathways in rats with 5/6 nephrectomy. *Kidney Int* 89: 1049–1061, 2016. doi:10.1016/j.kint.2016.01.016.
23. **Delic D, Wiech F, Urquhart R, Gabrielyan O, Rieber K, Rolser M, Tsuprykov O, Hasan AA, Kramer BK, Baum P, Kohler A, Gantner F, Mark M, Hocher B, Klein T.** Linagliptin and telmisartan induced effects on renal and urinary exosomal miRNA expression in rats with 5/6 nephrectomy. *Sci Rep* 10: 3373, 2020. doi:10.1038/s41598-020-60336-4.
24. **Zeng S, Delic D, Chu C, Xiong Y, Luo T, Chen X, Gaballa MMS, Xue Y, Chen X, Cao Y, Hasan AA, Stadermann K, Frankenreiter S, Yin L, Kramer BK, Klein T, Hocher B.** Antifibrotic effects of low dose SGLT2 Inhibition with empagliflozin in comparison to Ang II receptor blockade with telmisartan in 5/6 nephrectomised rats on high salt

diet. *Biomed Pharmacother* 146: 112606, 2022. doi:10.1016/j.biopha.2021.112606.
25. **Sarashina A, Koiwai K, Seman LJ, Yamamura N, Taniguchi A, Negishi T, Sesoko S, Woerle HJ, Dugi KA.** Safety, tolerability, pharmacokinetics and pharmacodynamics of single doses of empagliflozin, a sodium glucose cotransporter 2 (SGLT2) inhibitor, in healthy Japanese subjects. *Drug Metab Pharmacokinet* 28: 213–219, 2013. doi:10.2133/dmpk.dmpk-12-rg-082.
26. **Grempler R, Thomas L, Eckhardt M, Himmelsbach F, Sauer A, Sharp DE, Bakker RA, Mark M, Klein T, Eickelmann P.** Empagliflozin, a novel selective sodium glucose cotransporter-2 (SGLT-2) inhibitor: characterisation and comparison with other SGLT-2 inhibitors. *Diabetes Obes Metab* 14: 83–90, 2012. doi:10.1111/j.1463-1326.2011.01517.x.
27. **Rajasekeran H, Lytvyn Y, Bozovic A, Lovshin JA, Diamandis E, Cattran D, Husain M, Perkins BA, Advani A, Reich HN, Kulasingam V, Cherney DZI.** Urinary adenosine excretion in type 1 diabetes. *Am J Physiol Renal Physiol* 313: F184–F191, 2017. doi:10.1152/ajprenal.00043.2017.
28. **Dias BCL, Fachi MM, de Campos ML, Degaut FLD, Peccinini RG, Pontarolo R.** A new HPLC-MS/MS method for the simultaneous quantification of SGLT2 inhibitors and metformin in plasma and its application to a pharmacokinetic study in healthy volunteers. *Biomed Chromatogr* 33: e4663, 2019. doi:10.1002/bmc.4663.
29. **Zeng S, Delic D, Chu C, Xiong Y, Luo T, Chen X, Gaballa MMS, Xue Y, Chen X, Cao Y, Hasan AA, Stadermann K, Frankenreiter S, Yin L, Kramer BK, Klein T, Hocher B.** Antifibrotic effects of low dose SGLT2 Inhibition with empagliflozin in comparison to Ang II receptor blockade with telmisartan in 5/6 nephrectomised rats on high salt diet. *Biomed Pharmacother* 146: 112606, 2022. doi:10.1016/j.biopha.2021.112606.
30. **Kanasaki K, Shi S, Kanasaki M, He J, Nagai T, Nakamura Y, Ishigaki Y, Kitada M, Srivastava SP, Koya D.** Linagliptin-mediated DPP-4 inhibition ameliorates kidney fibrosis in streptozotocin-induced diabetic mice by inhibiting endothelial-to-mesenchymal transition in a therapeutic regimen. *Diabetes* 63: 2120–2131, 2014. doi:10.2337/db13-1029.
31. **Winiarska A, Knysak M, Nabrdalik K, Gumprecht J, Stompor T.** Inflammation and oxidative stress in diabetic kidney disease: the targets for SGLT2 inhibitors and GLP-1 receptor agonists. *Int J Mol Sci* 22: 10822, 2021. doi:10.3390/ijms221910822.
32. **DeFronzo RA, Reeves WB, Awad AS.** Pathophysiology of diabetic kidney disease: impact of SGLT2 inhibitors. *Nat Rev Nephrol* 17: 319–334, 2021. doi:10.1038/s41581-021-00393-8.
33. **Lu YP, Wu HW, Zhu T, Li XT, Zuo J, Hasan AA, Reichetzeder C, Delic D, Yard B, Klein T, Kramer BK, Zhang ZY, Wang XH, Yin LH, Dai Y, Zheng ZH, Hocher B.** Empagliflozin reduces kidney fibrosis and improves kidney function by alternative macrophage activation in rats with 5/6-nephrectomy. *Biomed Pharmacother* 156: 113947, 2022. doi:10.1016/j.biopha.2022.113947.
34. **Wagner J, Drab M, Bohlender J, Amann K, Wienen W, Ganten D.** Effects of AT1 receptor blockade on blood pressure and the renin-angiotensin system in spontaneously hypertensive rats of the stroke prone strain. *Clin Exp Hypertens* 20: 205–221, 1998. doi:10.3109/10641969809053215.
35. **Te Riet L, van Esch JH, Roks AJ, van den Meiracker AH, Danser AH.** Hypertension: renin-angiotensin-aldosterone system alterations. *Circ Res* 116: 960–975, 2015. doi:10.1161/CIRCRESAHA.116.303587.
36. **Ahmed AS, Mona MM, Abdel-Kareem MA, Elsisy RA.** SGLT2 inhibitor empagliflozin monotherapy alleviates renal oxidative stress in albino Wistar diabetic rats after myocardial infarction induction. *Biomed Pharmacother* 139: 111624, 2021. doi:10.1016/j.biopha.2021.111624.
37. **Abdel-Wahab AF, Bamagous GA, Al-Harizy RM, ElSawy NA, Shahzad N, Ibrahim IA, Ghamdi SSA.** Renal protective effect of SGLT2 inhibitor dapagliflozin alone and in combination with irbesartan in a rat model of diabetic nephropathy. *Biomed Pharmacother* 103: 59–66, 2018. doi:10.1016/j.biopha.2018.03.176.
38. **Domon A, Katayama K, Sato T, Tochigi Y, Tazaki H, Suzuki H.** Empagliflozin ameliorates symptoms of diabetes and renal tubular dysfunction in a rat model of diabetes with enlarged kidney (DEK). *PLoS One* 16: e0251135, 2021. doi:10.1371/journal.pone.0251135.
39. **Cassis P, Locatelli M, Cerullo D, Corna D, Buelli S, Zanchi C, Villa S, Morigi M, Remuzzi G, Benigni A, Zoja C.** SGLT2 inhibitor dapagliflozin limits podocyte damage in proteinuric nondiabetic nephropathy. *JCI Insight* 3: e98720, 2018. doi:10.1172/jci.insight.98720.
40. **Castoldi G, Carletti R, Ippolito S, Colzani M, Barzaghi F, Stella A, Zerbini G, Perseghin G, Zatti G, di Gioia CRT.** Sodium-glucose cotransporter 2 inhibition prevents renal fibrosis in cyclosporine nephropathy. *Acta Diabetol* 58: 1059–1070, 2021. doi:10.1007/s00592-021-01681-2.
41. **Yamato M, Kato N, Kakino A, Yamada KI, Inoguchi T.** Low dose of sodium-glucose transporter 2 inhibitor ipragliflozin attenuated renal dysfunction and interstitial fibrosis in adenine-induced chronic kidney disease in mice without diabetes. *Metabol Open* 7: 100049, 2020. doi:10.1016/j.metop.2020.100049.
42. **Abbas NAT, El Salem A, Awad MM.** Empagliflozin, SGLT2 inhibitor, attenuates renal fibrosis in rats exposed to unilateral ureteric obstruction: potential role of klotho expression. *Naunyn Schmiedebergs Arch Pharmacol* 391: 1347–1360, 2018. doi:10.1007/s00210-018-1544-y.
43. **Kim S, Jo CH, Kim GH.** Effects of empagliflozin on nondiabetic salt-sensitive hypertension in uninephrectomized rats. *Hypertens Res* 42: 1905–1915, 2019. doi:10.1038/s41440-019-0326-3.
44. **Li L, Konishi Y, Morikawa T, Zhang Y, Kitabayashi C, Kobara H, Masaki T, Nakano D, Hitomi H, Kobori H, Nishiyama A.** Effect of a SGLT2 inhibitor on the systemic and intrarenal renin-angiotensin system in subtotally nephrectomized rats. *J Pharmacol Sci* 137: 220–223, 2018. doi:10.1016/j.jphs.2017.10.006.
45. **Zhang Y, Thai K, Kepecs DM, Gilbert RE.** Sodium-glucose linked cotransporter-2 inhibition does not attenuate disease progression in the rat remnant kidney model of chronic kidney disease. *PLoS One* 11: e0144640, 2016. doi:10.1371/journal.pone.0144640.
46. **Ku EJ, Lee DH, Jeon HJ, Oh TK.** Empagliflozin versus dapagliflozin in patients with type 2 diabetes inadequately controlled with metformin, glimepiride and dipeptidyl peptide 4 inhibitors: a 52-week prospective observational study. *Diabetes Res Clin Pract* 151: 65–73, 2019. doi:10.1016/j.diabres.2019.04.008.
47. **Ku EJ, Lee DH, Jeon HJ, Oh TK.** Long-term effectiveness and safety of quadruple combination therapy with empagliflozin versus dapagliflozin in patients with type 2 diabetes: 3-year prospective observational study. *Diabetes Res Clin Pract* 182: 109123, 2021. doi:10.1016/j.diabres.2021.109123.
48. **Tauber P, Sinha F, Berger RS, Gronwald W, Dettmer K, Kuhn M, Trum M, Maier LS, Wagner S, Schweda F.** Empagliflozin reduces renal hyperfiltration in response to uninephrectomy, but is not nephroprotective in UNx/DOCA/salt mouse models. *Front Pharmacol* 12: 761855, 2021. doi:10.3389/fphar.2021.761855.
49. **Corremans R, Neven E, Maudsley S, Leysen H, De Broe ME, D'Haese PC, Vervaet BA, Verhulst A.** Progression of established non-diabetic chronic kidney disease is halted by metformin treatment in rats. *Kidney Int* 101: 929–944, 2022. doi:10.1016/j.kint.2022.01.037.
50. **Perrone-Filardi P, Avogaro A, Bonora E, Colivicchi F, Fioretto P, Maggioni AP, Sesti G, Ferrannini E.** Mechanisms linking empagliflozin to cardiovascular and renal protection. *Int J Cardiol* 241: 450–456, 2017. doi:10.1016/j.ijcard.2017.03.089.
51. **Cherney DZ, Perkins BA, Soleymanlou N, Maione M, Lai V, Lee A, Fagan NM, Woerle HJ, Johansen OE, Broedl UC, von Eynatten M.** Renal hemodynamic effect of sodium-glucose cotransporter 2 inhibition in patients with type 1 diabetes mellitus. *Circulation* 129: 587–597, 2014. doi:10.1161/CIRCULATIONAHA.113.005081.
52. **Thurau K, Schnermann J.** The sodium concentration in the macula densa cells as a regulating factor for glomerular filtration (micropuncture experiments). *Klin Wochenschr* 43: 410–413, 1965. doi:10.1007/BF01483845.
53. **Oyarzun C, Garrido W, Alarcon S, Yanez A, Sobrevia L, Quezada C, San MR.** Adenosine contribution to normal renal physiology and chronic kidney disease. *Mol Aspects Med* 55: 75–89, 2017. doi:10.1016/j.mam.2017.01.004.
54. **Zehra T, Cupples WA, Braam B.** Tubuloglomerular feedback synchronization in nephrovascular networks. *J Am Soc Nephrol* 32: 1293–1304, 2021. doi:10.1681/ASN.2020040423.
55. **Fioretto P, Zambon A, Rossato M, Busetto L, Vettor R.** SGLT2 inhibitors and the diabetic kidney. *Diabetes Care* 39, *Suppl* 2: S165–171, 2016. doi:10.2337/dcS15-3006.
56. **Vallon V, Gerasimova M, Rose MA, Masuda T, Satriano J, Mayoux E, Koepsell H, Thomson SC, Rieg T.** SGLT2 inhibitor empagliflozin reduces renal growth and albuminuria in proportion to hyperglycemia and prevents glomerular hyperfiltration in diabetic Akita mice. *Am*

J Physiol Renal Physiol 306: F194–F204, 2014. doi:10.1152/ajprenal.00520.2013.

57. **Nordquist L, Brown R, Fasching A, Persson P, Palm F.** Proinsulin C-peptide reduces diabetes-induced glomerular hyperfiltration via efferent arteriole dilation and inhibition of tubular sodium reabsorption. *Am J Physiol Renal Physiol* 297: F1265–F1272, 2009. doi:10.1152/ajprenal.00228.2009.
58. **Persson P, Hansell P, Palm F.** Reduced adenosine A2a receptor-mediated efferent arteriolar vasodilation contributes to diabetes-induced glomerular hyperfiltration. *Kidney Int* 87: 109–115, 2015. doi:10.1038/ki.2014.219.
59. **Skrtic M, Cherney DZ.** Sodium-glucose cotransporter-2 inhibition and the potential for renal protection in diabetic nephropathy. *Curr Opin Nephrol Hypertens* 24: 96–103, 2015. doi:10.1097/MNH.0000000000000084.
60. **Kobori H, Mori H, Masaki T, Nishiyama A.** Angiotensin II blockade and renal protection. *Curr Pharm Des* 19: 3033–3042, 2013. doi:10.2174/1381612811319170009.
61. **Barnett AH.** Preventing renal complications in diabetic patients: the Diabetics Exposed to Telmisartan And enalaprIL (DETAIL) study. *Acta Diabetol* 42,Suppl1: S42–S49, 2005. doi:10.1007/s00592-005-0180-4.
62. **Kobori H, Nangaku M, Navar LG, Nishiyama A.** The intrarenal renin-angiotensin system: from physiology to the pathobiology of hypertension and kidney disease. *Pharmacol Rev* 59: 251–287, 2007. doi:10.1124/pr.59.3.3.
63. **Imanishi M, Yoshioka K, Konishi Y, Okumura M, Okada N, Sato T, Tanaka S, Fujii S, Kimura G.** Glomerular hypertension as one cause of albuminuria in type II diabetic patients. *Diabetologia* 42: 999–1005, 1999. doi:10.1007/s001250051259.
64. **Castrop H.** Mediators of tubuloglomerular feedback regulation of glomerular filtration: ATP and adenosine. *Acta Physiol (Oxf)* 189: 3–14, 2007. doi:10.1111/j.1748-1716.2006.01610.x.
65. **Osswald H, Muhlbauer B, Vallon V.** Adenosine and tubuloglomerular feedback. *Blood Purif* 15: 243–252, 1997. doi:10.1159/000170342.
66. **Carlstrom M, Wilcox CS, Welch WJ.** Adenosine A(2) receptors modulate tubuloglomerular feedback. *Am J Physiol Renal Physiol* 299: F412–F417, 2010. doi:10.1152/ajprenal.00211.2010.
67. **Persson AE, Lai EY, Gao X, Carlstrom M, Patzak A.** Interactions between adenosine, angiotensin II and nitric oxide on the afferent arteriole influence sensitivity of the tubuloglomerular feedback. *Front Physiol* 4: 187, 2013. doi:10.3389/fphys.2013.00187.
68. **Wanner C.** Sodium glucose cotransporter 2 inhibition and the visualization of kidney hemodynamics. *Circulation* 140: 316–318, 2019. doi:10.1161/CIRCULATIONAHA.119.040326.
69. **Marton A, Kaneko T, Kovalik JP, Yasui A, Nishiyama A, Kitada K, Titze J.** Organ protection by SGLT2 inhibitors: role of metabolic energy and water conservation. *Nat Rev Nephrol* 17: 65–77, 2021. doi:10.1038/s41581-020-00350-x.
70. **Kidokoro K, Cherney DZI, Bozovic A, Nagasu H, Satoh M, Kanda E, Sasaki T, Kashihara N.** Evaluation of glomerular hemodynamic function by empagliflozin in diabetic mice using in vivo imaging. *Circulation* 140: 303–315, 2019. doi:10.1161/CIRCULATIONAHA.118.037418.
71. **Vallon V, Verma S.** Effects of SGLT2 inhibitors on kidney and cardiovascular function. *Annu Rev Physiol* 83: 503–528, 2021. doi:10.1146/annurev-physiol-031620-095920.
72. **Castoldi G, Carletti R, Ippolito S, Colzani M, Barzaghi F, Stella A, Zerbini G, Perseghin G, di Gioia CRT.** Renal anti-fibrotic effect of sodium glucose cotransporter 2 inhibition in angiotensin II-dependent hypertension. *Am J Nephrol* 51: 119–129, 2020. doi:10.1159/000505144.
73. **Rajasekeran H, Reich HN, Hladunewich MA, Cattran D, Lovshin JA, Lytvyn Y, Bjornstad P, Lai V, Tse J, Cham L, Majumder S, Bowskill BB, Kabir MG, Advani SL, Gibson IW, Sood MM, Advani A, Cherney DZI.** Dapagliflozin in focal segmental glomerulosclerosis: a combined human-rodent pilot study. *Am J Physiol Renal Physiol* 314: F412–F422, 2018. doi:10.1152/ajprenal.00445.2017.
74. **Kishore U, Reid KB.** C1q: structure, function, and receptors. *Immunopharmacology* 49: 159–170, 2000. doi:10.1016/s0162-3109(00)80301-x.
75. **Muller-Eberhard HJ.** Molecular organization and function of the complement system. *Annu Rev Biochem* 57: 321–347, 1988. doi:10.1146/annurev.bi.57.070188.001541.
76. **Tang S, Sheerin NS, Zhou W, Brown Z, Sacks SH.** Apical proteins stimulate complement synthesis by cultured human proximal tubular epithelial cells. *J Am Soc Nephrol* 10: 69–76, 1999. doi:10.1681/ASN.V10169.
77. **Peng Q, Li K, Patel H, Sacks SH, Zhou W.** Dendritic cell synthesis of C3 is required for full T cell activation and development of a Th1 phenotype. *J Immunol* 176: 3330–3341, 2006. doi:10.4049/jimmunol.176.6.3330.
78. **Li K, Fazekasova H, Wang N, Peng Q, Sacks SH, Lombardi G, Zhou W.** Functional modulation of human monocytes derived DCs by anaphylatoxins C3a and C5a. *Immunobiology* 217: 65–73, 2012. doi:10.1016/j.imbio.2011.07.033.
79. **Bora PS, Sohn JH, Cruz JM, Jha P, Nishihori H, Wang Y, Kaliappan S, Kaplan HJ, Bora NS.** Role of complement and complement membrane attack complex in laser-induced choroidal neovascularization. *J Immunol* 174: 491–497, 2005. doi:10.4049/jimmunol.174.1.491.
80. **Huang G, Zhang Y, Kim B, Ge G, Annis DS, Mosher DF, Greenspan DS.** Fibronectin binds and enhances the activity of bone morphogenetic protein 1. *J Biol Chem* 284: 25879–25888, 2009. doi:10.1074/jbc.M109.024125.
81. **Xavier S, Sahu RK, Landes SG, Yu J, Taylor RP, Ayyadevara S, Megyesi J, Stallcup WB, Duffield JS, Reis ES, Lambris JD, Portilla D.** Pericytes and immune cells contribute to complement activation in tubulointerstitial fibrosis. *Am J Physiol Renal Physiol* 312: F516–F532, 2017. doi:10.1152/ajprenal.00604.2016.
82. **Portilla D, Xavier S.** Role of intracellular complement activation in kidney fibrosis. *Br J Pharmacol* 178: 2880–2891, 2021. doi:10.1111/bph.15408.

My curriculum vitae does not appear in the electronic version of my paper for reasons of data protection.

My curriculum vitae does not appear in the electronic version of my paper for reasons of data protection.

My curriculum vitae does not appear in the electronic version of my paper for reasons of data protection.

Publications list

1. **Chen, X.**, Delić, D., Cao, Y., Shen, L., Shao, Q., Zhang, Z., Wu, H., Hasan, A. A., Reichetzeder, C., Gaballa, M. M. S., Krämer, B. K., Klein, T., Yin, L., He, B., Morgera, S., & Hocher, B. (2023). Reno-protective Effects of Empagliflozin are linked to Activation of the Tubuloglomerular Feedback Mechanism and Blunting of the Complement System. American journal of physiology. Cell physiology, 10.1152/ajpcell.00528.2022. Advance online publication. https://doi.org/10.1152/ajpcell.00528.2022 (IF=5.282)

2. **Chen, X.**, Hocher, C. F., Shen, L., Krämer, B. K., & Hocher, B. (2023). Reno- and cardioprotective molecular mechanisms of SGLT2 inhibitors beyond glycemic control - from bedside to bench. American journal of physiology. Cell physiology, 10.1152/ajpcell.00177.2023. Advance online publication. https://doi.org/10.1152/ajpcell.00177.2023 (IF=5.282)

3. **Chen, X.**, Chu, C., Doebis, C., Xiong, Y., Cao, Y., Krämer, B. K., von Baehr, V., & Hocher, B. (2022). Vitamin D status and its association with parathyroid hormone in 23,134 outpatients. The Journal of steroid biochemistry and molecular biology, 220, 106101. https://doi.org/10.1016/j.jsbmb.2022.106101 (IF=5.011)

4. **Chen, X.**, Chu, C., Doebis, C., von Baehr, V., & Hocher, B. (2021). Sex-Dependent Association of Vitamin D With Insulin Resistance in Humans. The Journal of clinical endocrinology and metabolism, 106(9), e3739–e3747. https://doi.org/10.1210/clinem/dgab213 (IF=6.134)

5. **Chen, X.**, Lu, Y. P., Luo, T., Wu, H. W., Cai, S. F., Tian, M., Yin, L. H., Krämer, B. K., Liu, F. N., Hocher, B., & Elitok, S. (2019). Free 25-Vitamin D Is Correlated with Cardiovascular Events in Prevalent Hemodialysis Patients but Not with Markers of Renal Mineral Bone Disease. Kidney & blood pressure research, 44(3), 344–353. https://doi.org/10.1159/000499878 (IF=3.096)

6. Cao, Y., **Chen, X.**, & Sun, H. (2021). Silencing of O-linked N-acetylglucosamine transferase ameliorates hypercalcemia-induced neurotoxicity in renal failure by regulating EZH2/KLF2/CXCL1 axis. Cell death & disease, 12(9), 819. https://doi.org/10.1038/s41419-021-04022-x (IF=9.685)

7. Hocher, C. F., **Chen, X.**, Zuo, J., Horvathova, K., Hocher, B., Krämer, B. K., & Chu, C. (2023). Fibroblast growth factor 23 is associated with the development of gestational diabetes mellitus. Diabetes/metabolism research and reviews, e3704. Advance online publication. https://doi.org/10.1002/dmrr.3704 (IF=8.0)

8. Chu, C., **Chen, X.**, Hasan, A. A., Szakallova, A., Krämer, B. K., Tepel, M., & Hocher, B. (2022). Angiopoietin-2 predicts all-cause mortality in male but not female end-stage kidney disease patients on hemodialysis. Nephrology, dialysis, transplantation : official publication of the European

Dialysis and Transplant Association - European Renal Association, 37(7), 1348–1356. https://doi.org/10.1093/ndt/gfab332 (IF=7.186)

9. Tsuprykov, O., **Chen, X.**, Hocher, C. F., Skoblo, R., Lianghong Yin, & Hocher, B. (2018). Why should we measure free 25(OH) vitamin D?. The Journal of steroid biochemistry and molecular biology, 180, 87–104. https://doi.org/10.1016/j.jsbmb.2017.11.014 (IF=5.011)

10. Chu, C., Tsuprykov, O., **Chen, X.**, Elitok, S., Krämer, B. K., & Hocher, B. (2021). Relationship Between Vitamin D and Hormones Important for Human Fertility in Reproductive-Aged Women. Frontiers in endocrinology, 12, 666687. https://doi.org/10.3389/fendo.2021.666687 (IF=6.055)

11. Hocher, B., Schönbrunn, A., **Chen, X.**, Krämer, B. K., & von Baehr, V. (2022). Outliers Matter-Correlation between S1 IgG SARS-CoV-2 Antibodies and Neutralizing SARS-CoV-2 Antibodies. Microorganisms, 10(10), 2067. https://doi.org/10.3390/microorganisms10102067 (IF=4.926)

12. Zuo, J., Chaykovska, L., Chu, C., **Chen, X.**, Hasan, A. A., Krämer, B. K., Tepel, M., & Hocher, B. (2022). Head-to-Head Comparison of Oxidative Stress Biomarkers for All-Cause Mortality in Hemodialysis Patients. Antioxidants (Basel, Switzerland), 11(10), 1975. https://doi.org/10.3390/antiox11101975 (IF=7.675)

13. Xiong, Y., Delic, D., Zeng, S., **Chen, X.**, Chu, C., Hasan, A. A., Krämer, B. K., Klein, T., Yin, L., & Hocher, B. (2022). Regulation of SARS CoV-2 host factors in the kidney and heart in rats with 5/6 nephrectomy-effects of salt, ARB, DPP4 inhibitor and SGLT2 blocker. BMC nephrology, 23(1), 117. https://doi.org/10.1186/s12882-022-02747-1(IF=2.585)

14. Chu, C., Delić, D., Alber, J., Feger, M., Xiong, Y., Luo, T., Hasan, A. A., Zeng, S., Gaballa, M. M. S., **Chen, X.**, Yin, L., Klein, T., Elitok, S., Krämer, B. K., Föller, M., & Hocher, B. (2022). Head-to-head comparison of two SGLT-2 inhibitors on AKI outcomes in a rat ischemia-reperfusion model. Biomedicine & pharmacotherapy = Biomedecine & pharmacotherapie, 153, 113357. https://doi.org/10.1016/j.biopha.2022.113357 (IF=7.419)

15. Zeng, S., Delic, D., Chu, C., Xiong, Y., Luo, T., Chen, X., Gaballa, M. M. S., Xue, Y., **Chen, X.**, Cao, Y., Hasan, A. A., Stadermann, K., Frankenreiter, S., Yin, L., Krämer, B. K., Klein, T., & Hocher, B. (2022). Antifibrotic effects of low dose SGLT2 Inhibition with empagliflozin in comparison to Ang II receptor blockade with telmisartan in 5/6 nephrectomised rats on high salt diet. Biomedicine & pharmacotherapy = Biomedecine & pharmacotherapie, 146, 112606. https://doi.org/10.1016/j.biopha.2021.112606 (IF=7.419)

Acknowledgments

I would like to express my sincere gratitude to Charité – Universitätsmedizin and to my two supervisors, Prof. Berthold Hocher and Prof. Stanislao Morgera. I would like to thank them for giving me the opportunity to study at one of the world's leading universities, Charité – Universitätsmedizin. During the difficult times of the COVID-19 epidemic, they have given me endless help and encouragement in both life and research. They were always forward-thinking and patient when my research got stuck. Their profound knowledge and dedication to research has been very helpful to me during these years. Under their guidance over the past three years, I have not only learnt how to explore science, but more importantly, their dedication and passion for medicine has infected me in my quest to become a better doctor.

Furthermore, I would like to thank our group leader, Ahmed A. Hasan, for his patience in teaching me about the experiments and giving me constructive advice over the past three years. Many thanks to my friend Yaochen Cao for his support and encouragement throughout the research period. Thanks to Prof. Bernhard K. Krämer for his guidance on all my published clinical studies. I am grateful to all my friends and colleagues who have helped me during these three years, including Denis Delić, Thomas Klein, Carl-Friedrich Hocher, Christoph Reichetzeder, Mohamed M.S. Gaballa, Yingquan Xiong, Shufei Zeng, Chang Chu, Jiao Zuo, Xiaoli Zhang, Zheyu Zhang, Hongwei Wu, Xitong Li, Mei Li and Chenwei Piao. I feel very fortunate to have worked in our wonderful and friendly team. Many thanks to all the authors of this publication for their efforts.

In addition, I am sincerely grateful to my parents and grandparents for their unending support and understanding in my medical career. Their love has been my greatest moral support. I am grateful to my motherland for providing the scholarship.

Berlin, July 15, 2023

Xin Chen